NATIONAL ADVISORY COMMITTEE FOR AERONAUTICS

REPORT No. 791

A THEORETICAL INVESTIGATION OF LONGITUDINAL STABILITY OF AIRPLANES WITH FREE CONTROLS INCLUDING EFFECT OF FRICTION IN CONTROL SYSTEM

By HARRY GREENBERG and LEONARD STERNFIELD

1944

For sale by the Superintendent of Documents, U. S. Government Printing Office, Washington 25, D. C. Price 10 cents

DISCLAIMER NOTICE

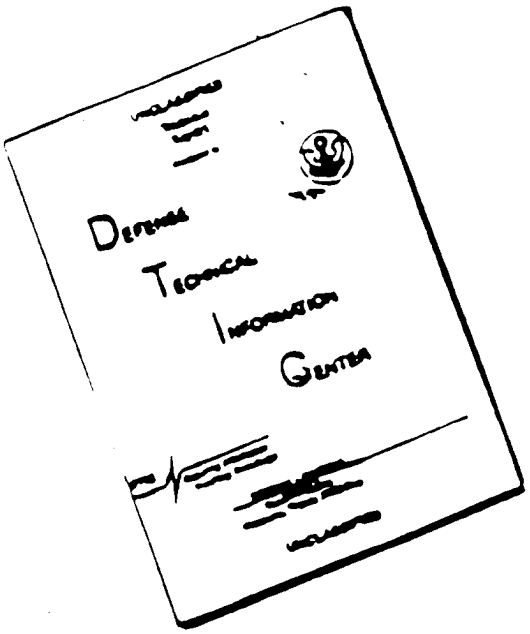

THIS DOCUMENT IS BEST QUALITY AVAILABLE. THE COPY FURNISHED TO DTIC CONTAINED A SIGNIFICANT NUMBER OF PAGES WHICH DO NOT REPRODUCE LEGIBLY.

AERONAUTIC SYMBOLS

1. FUNDAMENTAL AND DERIVED UNITS

	Symbol	Metric		English	
		Unit	Abbreviation	Unit	Abbreviation
Length	l	meter	m	foot (or mile)	ft (or mi)
Time	t	second	s	second (or hour)	sec (or hr)
Force	F	weight of 1 kilogram	kg	weight of 1 pound	lb
Power	P	horsepower (metric)		horsepower	hp
Speed	V	kilometers per hour	kph	miles per hour	mph
		meters per second	mps	feet per second	fps

2. GENERAL SYMBOLS

W Weight$=mg$

g Standard acceleration of gravity$=9.80665$ m/s^2 or 32.1740 ft/sec^2

m Mass$=\frac{W}{g}$

I Moment of inertia$=mk^2$. (Indicate axis of radius of gyration k by proper subscript.)

μ Coefficient of viscosity

ν Kinematic viscosity

ρ Density (mass per unit volume)

Standard density of dry air, 0.12497 kg-m^{-4}-s^2 at 15° C and 760 mm; or 0.002378 lb-ft^{-4} sec^2

Specific weight of "standard" air, 1.2255 kg/m^3 or 0.07651 lb/cu ft

3. AERODYNAMIC SYMBOLS

S Area

S_w Area of wing

G Gap

b Span

c Chord

A Aspect ratio, $\frac{b^2}{S}$

V True air speed

q Dynamic pressure, $\frac{1}{2}\rho V^2$

L Lift, absolute coefficient $C_L=\frac{L}{qS}$

D Drag, absolute coefficient $C_D=\frac{D}{qS}$

D_o Profile drag, absolute coefficient $C_{Do}=\frac{D_o}{qS}$

D_i Induced drag, absolute coefficient $C_{Di}=\frac{D_i}{qS}$

D_p Parasite drag, absolute coefficient $C_{Dp}=\frac{D_p}{qS}$

C Cross-wind force, absolute coefficient $C_C=\frac{C}{qS}$

i_w Angle of setting of wings (relative to thrust line)

i_t Angle of stabilizer setting (relative to thrust line)

Q Resultant moment

Ω Resultant angular velocity

R Reynolds number, $\rho\frac{Vl}{\mu}$ where l is a linear dimension (e.g., for an airfoil of 1.0 ft chord, 100 mph, standard pressure at 15° C, the corresponding Reynolds number is 935,400; or for an airfoil of 1.0 m chord, 100 mps, the corresponding Reynolds number is 6,865,000)

α Angle of attack

ϵ Angle of downwash

α_o Angle of attack, infinite aspect ratio

α_i Angle of attack, induced

α_a Angle of attack, absolute (measured from zero-lift position)

γ Flight-path angle

REPORT No. 791

A THEORETICAL INVESTIGATION OF LONGITUDINAL STABILITY OF AIRPLANES WITH FREE CONTROLS INCLUDING EFFECT OF FRICTION IN CONTROL SYSTEM

By HARRY GREENBERG and LEONARD STERNFIELD

Langley Memorial Aeronautical Laboratory
Langley Field, Va.

National Advisory Committee for Aeronautics

Headquarters, 1500 New Hampshire Avenue NW., Washington 25, D. C.

Created by act of Congress approved March 3, 1915, for the supervision and direction of the scientific study of the problems of flight (U. S. Code, title 49, sec. 241). Its membership was increased to 15 by act approved March 2, 1929. The members are appointed by the President, and serve as such without compensation.

TECHNICAL COMMITTEES

AERODYNAMICS

POWER PLANTS FOR AIRCRAFT

AIRCRAFT CONSTRUCTION

OPERATING PROBLEMS

MATERIALS RESEARCH COORDINATION

Coordination of Research Needs of Military and Civil Aviation

Preparation of Research Programs

Allocation of Problems

Prevention of Duplication

LANGLEY MEMORIAL AERONAUTICAL LABORATORY
Langley Field, Va.

AMES AERONAUTICAL LABORATORY
Moffett Field, Calif.

AIRCRAFT ENGINE RESEARCH LABORATORY, Cleveland Airport, Cleveland, Ohio

Conduct, under unified control, for all agencies, of scientific research on the fundamental problems of flight

---

OFFICE OF AERONAUTICAL INTELLIGENCE, Washington, D. C.

Collection, classification, compilation, and dissemination of scientific and technical information on aeronautics

REPORT No. 791

A THEORETICAL INVESTIGATION OF LONGITUDINAL STABILITY OF AIRPLANES WITH FREE CONTROLS INCLUDING EFFECT OF FRICTION IN CONTROL SYSTEM

By Harry Greenberg and Leonard Sternfield

SUMMARY

The relation between the elevator hinge-moment parameters and the control forces for changes in forward speed and in maneuvers is shown for several values of static stability and elevator mass balance.

The stability of the short-period oscillations is shown as a series of boundaries giving the limits of the stable region in terms of the elevator hinge-moment parameters. The effects of static stability, elevator moment of inertia, elevator mass unbalance, and airplane density are also considered. Dynamic instability is likely to occur if there is mass unbalance of the elevator control system combined with a small restoring tendency (high aerodynamic balance). This instability can be prevented by a rearrangement of the unbalancing weights which, however, involves an increase of the amount of weight necessary. It can also be prevented by the addition of viscous friction to the elevator control system provided the airplane center of gravity is not behind a certain critical position.

For high values of the density parameter, which correspond to high altitudes of flight, the addition of moderate amounts of viscous friction may be destabilizing even when the airplane is statically stable. In this case, increasing the viscous friction makes the oscillation stable again. The condition in which viscous friction causes dynamic instability of a statically stable airplane is limited to a definite range of hinge-moment parameters. It is shown that, when viscous friction causes increasing oscillations, solid friction will produce steady oscillations having an amplitude proportional to the amount of friction.

INTRODUCTION

The effects of aerodynamic balance and mass unbalance of the elevator on the dynamic stability of the airplane are discussed in a previous report on control-free stability (reference 1). It was found theoretically in reference 1 and verified in flight (reference 2) that, if the elevator is too closely balanced aerodynamically and has a sufficient amount of mass unbalance (which tends to depress the elevator), increasing oscillations of short period may occur. Other flight tests (reference 3) showed, however, that mass unbalance of the elevator control system improves the static stability of an airplane, that is, increases the slope of the curve of stick force against speed in level flight and of the curve of stick force against normal acceleration in maneuvers. Subsequent work (reference 4) has indicated that a control surface with positive floating tendency (tendency to float against the relative wind), when used as a rudder, is effective in improving control-free static stability. A theoretical analysis (reference 5) showed that a rudder having a positive floating ratio may, under the influence of solid friction in the control system, build up steady oscillations of the airplane and rudder. These steady oscillations have been observed in flight tests (reference 6). These results suggested an investigation of the behavior of an airplane equipped with an elevator having a positive floating tendency. This type of elevator was not considered in any of the previous investigations.

The purpose of the present report is to make a theoretical analysis of the control-free longitudinal stability of an airplane, which takes account of this current trend toward a positive floating tendency in control-surface design and covers, in general, a much wider range of parameters than the investigation of reference 1. These parameters include, for the elevator control system, restoring tendency, floating tendency, mass unbalance (bobweight control), moment of inertia, and viscous and solid friction and, for the airplane, density and center-of-gravity position.

The method of analysis of dynamic stability is based on the classical theory of Bryan and Bairstow extended to include movements of the controls and their couplings with the airplane motions. Friction is treated in the same way as in the approximate method of reference 5, in which solid friction is replaced by an equivalent viscous friction.

Before the analysis of dynamic stability is presented, some discussion is given of the effect of the various parameters on the elevator forces for trim and for acceleration—characteristics considered important to flying qualtities. The stability of the short-period oscillations, with and without friction in the control system, is then considered. The effects of weights added to the system to modify the static and dynamic stability are discussed. The trends to be expected are illustrated by a series of calculations and charts based on a typical airplane. The stability of the long-period (phugoid) oscillations is not discussed because of its relative unimportance.

SYMBOLS

A_w wing aspect ratio

A_t tail aspect ratio

A, B, C, E, F coefficients in stability equation

b wing span

C_h elevator hinge-moment coefficient $\left(\frac{H}{\frac{1}{2}\rho V^2 S_e c_e}\right)$

C_{h_f} frictional hinge-moment coefficient $\left(\frac{H_f}{\frac{1}{2}\rho V^2 S_e c_e}\right)$

C_{h_0} applied hinge-moment coefficient

C_L airplane lift coefficient $\left(\frac{\text{Lift}}{qS_w}\right)$

C_{L_t} lift coefficient of tail

C_m pitching-moment coefficient about airplane center of gravity

c wing chord

c_e elevator chord

D differential operator $\left(\frac{d}{ds}\right)$

F constant term in stability equation

F_s stick force; positive for pull

F_n stick-force gradient in maneuvers $\left(\frac{dF_s}{dn}\right)$

F_u stick-force gradient for level flight $\left(\frac{dF_s}{du}\right)$

g acceleration of gravity

H hinge moment; positive when tends to depress trailing edge

H_e mass moment of elevator about its hinge; positive when tailheavy

H_s mass moment of control stick about its pivot; positive when stick tends to move forward

H_f frictional hinge moment

$H_0 = H_e + rH_s$

$h = rh_s + h_e$

$h_e = \frac{4H_e}{\rho S_e c_e c}$

$h_s = \frac{4H_s}{\rho S_e c_e c}$

I_e moment of inertia of elevator about its hinge

I_s moment of inertia of control stick about its pivot

$i_1 = i_e - ri_s$

$i_2 = i_e + r^2 i_s$

$i_e = \frac{8I_e}{\rho S_e c_e c^2}$

$= \frac{8I_s}{\rho S_e c_e c^2}$

k_Y radius of gyration of airplane about Y-axis

$k_y = \frac{2k_Y}{c}$

L_h distance between airplane center of gravity and elevator hinge

$l_h = \frac{2L_h}{c}$

l length of control stick

M pitching moment about airplane center of gravity

m mass of airplane

$N_{1/2}$ number of cycles required for oscillation to damp to half amplitude

n normal acceleration per g of airplane due to curvature of flight path; accelerometer reading minus component of gravity force

P period of oscillation, seconds

q dynamic pressure

S elevator area

S_t tail area

S_w wing area

s distance in half-chords $(2Vt/c)$

$T_{1/2}$ time required for oscillation to damp to half amplitude, seconds

t time

$u = \frac{\Delta V}{V}$

V forward velocity

ΔV change in forward velocity from trimmed value

W weight of airplane

X longitudinal force; positive forward

$x_{a.c.}$ distance of center of gravity from aerodynamic center; positive when center of gravity is ahead of aerodynamic center

Z normal force; positive downward

α angle of attack

α_t angle of attack at tail

δ_e deflection of elevator; positive for downward motion of trailing edge

$\bar{\delta}$ amplitude of elevator oscillation

ϵ angle of downwash

r control gearing (θ_s/δ_e)

θ angle of pitch of airplane

θ_s deflection of control stick; positive for forward motion of stick

λ complex root of stability equation

ξ, η real and imaginary parts, respectively, of λ

μ airplane-density parameter $(m/\rho S_w b)$

ρ mass density of air

Whenever u, V, α, α_t, θ, δ, $D\alpha$, $D\theta$, $D\delta$, and $D^2\alpha$ are used as subscripts, a derivative is indicated. For example, $X_V = \frac{\partial X}{\partial V}$ and $C_{h_{D\delta}} = \frac{\partial C_h}{\partial D\delta}$. Whenever a dot is used above a symbol, it denotes differentiation with respect to time.

All angles are measured in radians.

METHOD OF ANALYSIS

Four degrees of freedom—forward speed, angle of attack, angle of pitch, and elevator deflection—are generally involved in the problem of control-free stability. To each degree of freedom, there corresponds an equation of equilibrium between inertial and aerodynamic forces or moments. By use of wind axes, the four equations become, for level flight,

$$
\begin{aligned}
&X_V\Delta V+X_\alpha\alpha && +X_\theta\theta && = m\Delta\dot{V}\\
&Z_V\Delta V-Z_\alpha\alpha && && = mV(\dot{\alpha}-\theta)\\
&M_V\Delta V+M_\alpha\alpha+M_{\dot{\alpha}}\dot{\alpha}+M_{\ddot{\alpha}}\ddot{\alpha} && +M_{\dot{\theta}}\dot{\theta}+M_\theta\theta+M_{\delta_e}\delta_e+M_{\dot{\delta}_e}\dot{\delta}_e = mk_Y^2\ddot{\theta}\\
&H_V\Delta V-H_\alpha\alpha+H_{\dot{\alpha}}\dot{\alpha}+H_{\ddot{\alpha}}\ddot{\alpha} && +H_{\dot{\theta}}\dot{\theta}+H_\theta\theta-H_{\delta_e}\delta_e-H_{\dot{\delta}_e}\dot{\delta}_e-I_e(\ddot{\theta}+\ddot{\delta}_e)-H_{\dot{\alpha}}(V\dot{\alpha}-V\dot{\theta}+L_h\ddot{\theta})+r[I_s(r\ddot{\delta}_e-\ddot{\theta})+H_{\dot{\alpha}}(V\dot{\alpha}-V\dot{\theta})]
\end{aligned}
$$

which can be written in nondimensional form as

$$
\left.
\begin{aligned}
&(-x_u+2A_w\mu D)u-x_\alpha\alpha && +\frac{C_L}{2}\theta && =0\\
&C_Lu+\left(\frac{C_{L_\alpha}}{2}+2A_w\mu D\right)\alpha && -2A_w\mu D\theta && =0\\
&C_{m_u}u+(C_{m_\alpha}+C_{m_{D\alpha}}D+C_{m_{D^2\alpha}}D^2)\alpha && +(C_{m_{D\theta}}D-2A_w\mu k_Y^2D^2)\theta && +(C_{m_\delta}+C_{m_{D\delta}}D)\delta_e =0\\
&C_{h_u}u+(C_{h_\alpha}+C_{h_{D\alpha}}D-hD+C_{h_{D^2\alpha}}D^2)\alpha+(C_{h_{D\theta}}D+hD-h_ch_hD^2-i_1D^2)\theta+(C_{h_\delta}+C_{h_{D\delta}}D-i_2D^2)\delta_e=0
\end{aligned}
\right\} \quad (1)
$$

In applying equations (1) to dynamic stability, certain approximations may be made. For instance, short-period oscillations (of the order of 1 sec) involve negligible changes in forward speed, which may therefore be neglected in studying the short-period oscillations. In fact, the period and damping of these oscillations can be obtained to a high degree of accuracy by using only the last three of the equations (1) and setting $u=0$.

Equations (1) then become

$$
\left.
\begin{aligned}
&\left(\frac{C_{L_\alpha}}{2}+2A_w\mu D\right)\alpha && -2A_w\mu D\theta && =0\\
&(C_{m_\alpha}+C_{m_{D\alpha}}D+C_{m_{D^2\alpha}}D^2)\alpha && +(C_{m_{D\theta}}-2A_w\mu k_Y^2D)D\theta && +(C_{m_\delta}+C_{m_{D\delta}}D)\delta_e =0\\
&[C_{h_\alpha}+(C_{h_{D\alpha}}-h)D+C_{h_{D^2\alpha}}D^2]\alpha && +[C_{h_{D\theta}}+h-(h_ch_h+i_1)D]D\theta && +(C_{h_\delta}+C_{h_{D\delta}}D-i_2D^2)\delta_e=0
\end{aligned}
\right\} \quad (2)
$$

By setting

$$\alpha=\alpha_0e^{\lambda t} \qquad D\theta=(D\theta)_0e^{\lambda t} \qquad \delta_e=\delta_{e_0}e^{\lambda t}$$

it can be shown (reference 7) that λ must be a root of a quartic equation formed by writing

$$
\begin{vmatrix}
\frac{C_{L_\alpha}}{2}+2A_w\mu\lambda & -2A_w\mu & 0\\
C_{m_\alpha}+C_{m_{D\alpha}}\lambda+C_{m_{D^2\alpha}}\lambda^2 & C_{m_{D\theta}}-2A_w\mu k_Y^2\lambda & C_{m_\delta}+C_{m_{D\delta}}\lambda\\
C_{h_\alpha}+(C_{h_{D\alpha}}-h)\lambda+C_{h_{D^2\alpha}}\lambda^2 & C_{h_{D\theta}}+h-(h_ch_h+i_1)\lambda & C_{h_\delta}+C_{h_{D\delta}}\lambda-i_2\lambda^2
\end{vmatrix}
=0
$$

The resulting stability equation may be written as

$$A\lambda^4+B\lambda^3+C\lambda^2+E\lambda+F=0 \quad (3)$$

where A, B, C, E, and F are functions of the stability derivatives.

The study of the effects of different parameters on the control-free stability was made by a series of computations for an average airplane having the characteristics given hereinafter. The current trend toward a positive floating tendency in control-surface design suggests the use of $C_{h_{\alpha_t}}$ and C_{h_δ} as the fundamental variables to be used in expressing stability and control characteristics. The results are presented as a series of figures that show the relations between $C_{h_{\alpha_t}}$ and C_{h_δ} which, with the other derivatives fixed, satisfy the conditions for neutral dynamic stability and neutral static stability.

A curve for neutral dynamic stability is the boundary dividing the region of increasing oscillations from the region of damped oscillations and is obtained from Routh's discriminant

$$BCE-AE^2-FB^2=0$$

The condition for neutral static stability is that

$$F=0$$

The stability equation (3) has four roots. A pair of complex roots indicates an oscillatory mode and a real root indicates an aperiodic mode. The real part of the complex root determines the damping; the imaginary part determines the period of the oscillations. More specifically, if there is a pair of complex roots

$$\lambda=\xi\pm i\eta$$

the period in seconds is given by

$$P = \frac{c}{2V}\cdot\frac{2\pi}{\eta}$$

and the time in seconds to damp to half amplitude is given by

$$T_{1/2} = -\frac{c}{2V}\cdot\frac{0.693}{\xi}$$

For an airplane at constant speed, there may be two oscillatory modes, there may be only one oscillatory mode, or the motion may be entirely aperiodic. In cases in which there are oscillatory components, one of the oscillations may be poorly damped and even become unstable.

The average airplane on which the calculations of this report are based is of conventional design. The characteristics of the airplane are

A_w	6
k_y	1.5
$\frac{l_h}{c}=\frac{l_h}{2}$	3.3
r	1
S_t/S_w	0.18
l_s, ft	2
S_e/S_t	0.55
A_t	4.5

The basic stability derivatives and parameters obtained from these airplane characteristics by methods shown in appendix A are

C_{L_α}	4.3	$C_{m_{D\delta}}$	-15.3
$C_{L_{t_{\alpha_t}}}$	3.8	$C_{m_{D\alpha}}$	-8.9
ϵ_α	0.486	$C_{h_{D\alpha}}$	$3.22C_{h_{\alpha_t}}$
C_{m_δ}	-1.54	$C_{m_{D^2\alpha}}$	23.2
$C_{m_{D\delta}}$	-0.97	$C_{h_{D^2\alpha}}$	$-10.55C_{h_{\alpha_t}}$
$C_{h_{D\delta}}$ (with no friction)	-1		

The following parameters of the airplane were varied:

μ airplane-density parameter

C_{m_α} control-fixed static-stability parameter

The following parameters of the elevator control system were varied:

$C_{h_{\alpha_t}}$ floating tendency

C_{h_δ} restoring tendency

$C_{h_{D\delta}}$ elevator-damping parameter

i_e moment-of-inertia parameter of elevator about its hinge

i_s moment-of-inertia parameter of control stick about its hinge

h mass-moment parameter of elevator control system about elevator hinge

h_e mass-moment parameter of elevator alone about its hinge

As has been pointed out, the stability boundaries were plotted, in most cases, in terms of $C_{h_{\alpha_t}}$ and C_{h_δ} as the variables of the coordinate system. In analyzing the effects of friction in the control system, C_{h_δ} and $C_{h_{D\delta}}$ were used as the plotted variables in some figures whereas $C_{h_{\alpha_t}}$ and C_{h_δ} were used in others. The effect of the other parameters is found by varying them one at a time, through a range of values, and showing for each parameter a series of stability boundaries.

The size of the airplane, wing loading, and altitude are combined in the parameter μ, which is $\frac{m}{\rho S_w b}$. A variation in μ thus could be due to a variation in size, wing loading, or altitude, or any combination of these. The range of values of μ covered in the present report and some typical corresponding values of wing loading, altitude, and size are given in the following table:

μ	Wing loading (lb/sq ft)	Altitude (ft)	Mean wing chord (ft)
4.17	40	Sea level	21
12.5	40	Sea level	7
37.5	40	33,000	7

The range of C_{m_α} and the corresponding center-of-gravity positions are as follows:

C_{m_α}	$\frac{x_{a.c.}}{c}$ (fraction of mean wing chord)
-0.232	0.05
0	0
.232	$-.05$

The ranges of values of the other parameters, for a small airplane (chord, 7 ft), are as follows:

i_e and i_s	Moment of inertia of elevator control system (slug-ft²)
0	0
2	1.6
4	3.2

h	Stick force (lb)	
	At sea level	At 33,000 ft
0	0	0
10	37	12.5

$C_{h_{D\delta}}$	$\frac{dH/d\delta}{V}$ (lb-ft/100 mph/deg sec)	
	At sea level	At 33,000 ft
-10	5.85	1.95
-100	58.5	19.5

STATIC STABILITY AND RELATION TO CONTROL FORCES

The connection between the static stability and the airplane and control parameters is established to assist in the interpretation of the results obtained hereinafter. Equations (1) can be applied to static stability by setting all terms containing D and D^2 equal to zero and solving the

resulting equations simultaneously for the variation in forward speed with an applied elevator hinge moment. For level flight, θ is also zero and the resulting equations are

$$C_L u + \frac{C_{L_\alpha}}{2}\alpha = 0$$

$$C_{m_u} u + C_{m_\alpha}\alpha + C_{m_\delta}\delta_e = 0$$

$$C_{h_u} u + C_{h_\alpha}\alpha + C_{h_\delta}\delta_e = -C_{h_0}$$

Solving gives

$$-\frac{C_{h_0}}{u} = \frac{2\left(C_L C_{m_\alpha} C_{h_\delta} - C_L C_{h_\alpha} C_{m_\delta} + C_{m_\delta} C_{L_\alpha}\frac{C_{h_u}}{2} - C_{h_\delta} C_{m_u}\frac{C_{L_\alpha}}{2}\right)}{C_{L_\alpha} C_{m_\delta}}$$

The variation of stick force with fractional change in forward speed is

$$F_u = \frac{dF_s}{d(\Delta V/V)} = \frac{II}{l_s r u} = -\frac{C_{h_0} g S_e c_e}{l_s r u} = \frac{\rho S_e c_e c g A_{m}\mu}{l_s r C_L}\left(-\frac{C_{h_0}}{u}\right)$$

If effects of slipstream on the tail are neglected, $C_{m_u} = 0$. As shown in appendix A, $C_{h_u} = -\frac{hC_L}{2A_m\mu}$. Inserting these values in the expression for C_{h_0}/u shows that F_u is independent of forward speed.

The variation of control force with normal acceleration in a steady pull-up, with no change assumed in forward speed (see reference 8), can be found from equations (2) by equating to zero all terms containing D except $D\theta$. This procedure implies that the normal acceleration is due entirely to curvature of the flight path $D\theta$. The equations become, for an applied hinge moment,

$$\frac{C_{L_\alpha}}{2}\alpha - 2A_m\mu D\theta = 0$$

$$C_{m_\alpha}\alpha + C_{m_{D\theta}} D\theta + C_{m_\delta}\delta_e = 0$$

$$C_{h_\alpha}\alpha + (C_{h_{D\theta}} + h) D\theta + C_{h_\delta}\delta_e = -C_{h_0}$$

from which

$$-\frac{C_{h_0}}{D\theta} = \frac{4A_u\mu C_{h_\alpha} C_{m_\delta} + hC_{L_\alpha} C_{m_\delta} + C_{h_{D\theta}} C_{L_\alpha} C_{m_\delta} - 4A_m\mu C_{h_\delta} C_{m_\alpha} - C_{h_\delta} C_{m_{D\theta}} C_{L_\alpha}}{C_{L_\alpha} C_{m_\delta}}$$

If the normal acceleration is ng,

$$D\theta = \frac{cng}{2V^2}$$

and

$$F_n = \frac{dF_s}{dn} = -\frac{C_{h_0}\frac{1}{2}\rho V^2 S_e c_e c g}{2V^2 D\theta\, l_s r}$$

$$= -\frac{C_{h_0}}{D\theta}\frac{\rho S_e c_e c g}{4 l_s r}$$

These formulas for F_u and F_n are equivalent to equation (1) of reference 9 and equations (27) and (28) of reference 10.

The formulas indicate that the stick-force gradients F_u and F_n are dependent on most of the aforementioned airplane and elevator parameters. Figures 1 to 5 show the variation of these stick-force gradients with the parameters $C_{h_{\alpha_t}}$, C_{h_δ}, C_{m_α}, h, and μ. The gradients are independent of speed, although only within the limits of the assumptions made in the analysis, namely, neglect of power and of compressibility effects. The gradient F_u can be used to get the stick force for only a small change in forward speed because the stick force is not directly proportional to the change in speed. The stick force in a steady pull-up F_n, however, is proportional to the normal acceleration provided the control deflection is not so great that the basic assumption of linearity is violated.

The line $F_u = 0$ is the boundary for true static stability—that is, $F_u = 0$ is the condition for zero variation in stick force with forward speed in steady flight. This condition is the same as that obtained by setting $F = 0$, where F is the constant term of the sixth-order stability equation obtained from equations (1). On subsequent figures it is called the divergence boundary. The line $F_n = 0$ is the boundary for apparent static (or maneuvering) stability and is the condition for zero variation in stick force in a steady pull-up. This condition for $F_n = 0$ is obtained by setting $F = 0$ in the approximate stability equation (equations (3)), which is for three degrees of freedom (α, $D\theta$, and δ_e). On the unstable side of $F_u = 0$, a slow divergence occurs that is noticed by the pilot as an unstable variation of stick force with forward speed. The stick force due to normal acceleration in a pull-up is stable, however, unless the conditions are such that the airplane is operating on the unstable side of $F_n = 0$.

Figures 1 to 5 indicate that the parameters have the same effect on F_u and F_n except that the altitude affects only F_n. They show that the stick-force gradients on an airplane of given tail size and center-of-gravity position may be increased by making the floating tendency $C_{h_{\alpha_t}}$ more positive or by mass unbalancing the elevator control system to depress the elevator (make it tailheavy). The effect of the restoring tendency C_{h_δ} on the stick-force gradients depends on the relative position of the center of gravity and the aerodynamic center. If the center of gravity is ahead of the aerodynamic center (airplane stable with controls fixed), increasing the magnitude of C_{h_δ} increases the stick-force gradients. If the center of gravity is behind the aerodynamic center, this effect on F_u is reversed; the effect on F_n is not reversed, however, until the center of gravity is well behind the aerodynamic center (in this case, about 0.05c at sea level and 0.02c at 30,000 feet). If $C_{h_\delta} = 0$, the stick forces are independent of the position of the airplane center of gravity.

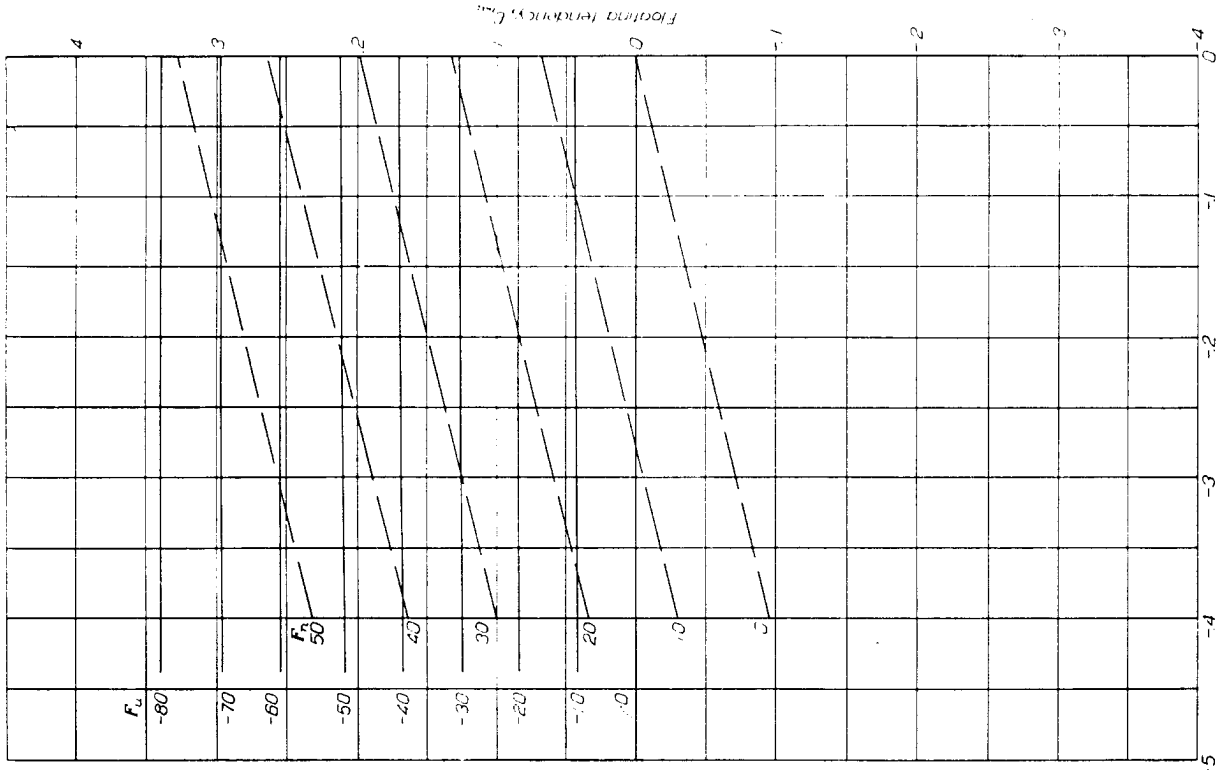

FIGURE 2.—Trim force F_s and pull-up force F_s as functions of hinge-moment parameters. $\tau_{a.c.}=0$; $\frac{W}{S_e}=40$ pounds per square foot; $c=7$ feet; sea level. F_s=stick force in pounds for $\frac{\Delta V}{V}=1.0$; F_s=stick force in pounds per g normal acceleration.

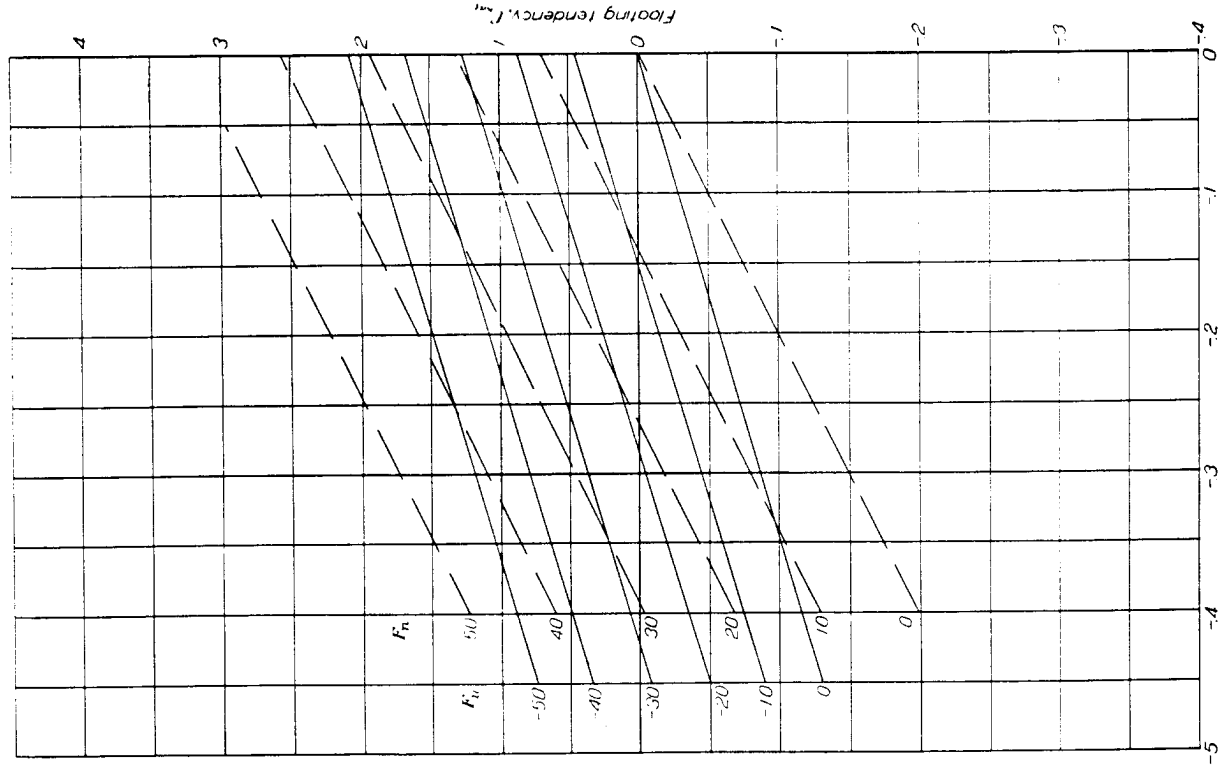

FIGURE 1.—Trim force F_s and pull-up force F_s as functions of hinge-moment parameters. $\tau_{a.c.}=0.05$; $\frac{W}{S_e}=40$ pounds per square foot; $c=7$ feet; sea level. F_s=stick force in pounds for $\frac{\Delta V}{V}=1.0$; F_s=stick force in pounds per g normal acceleration.

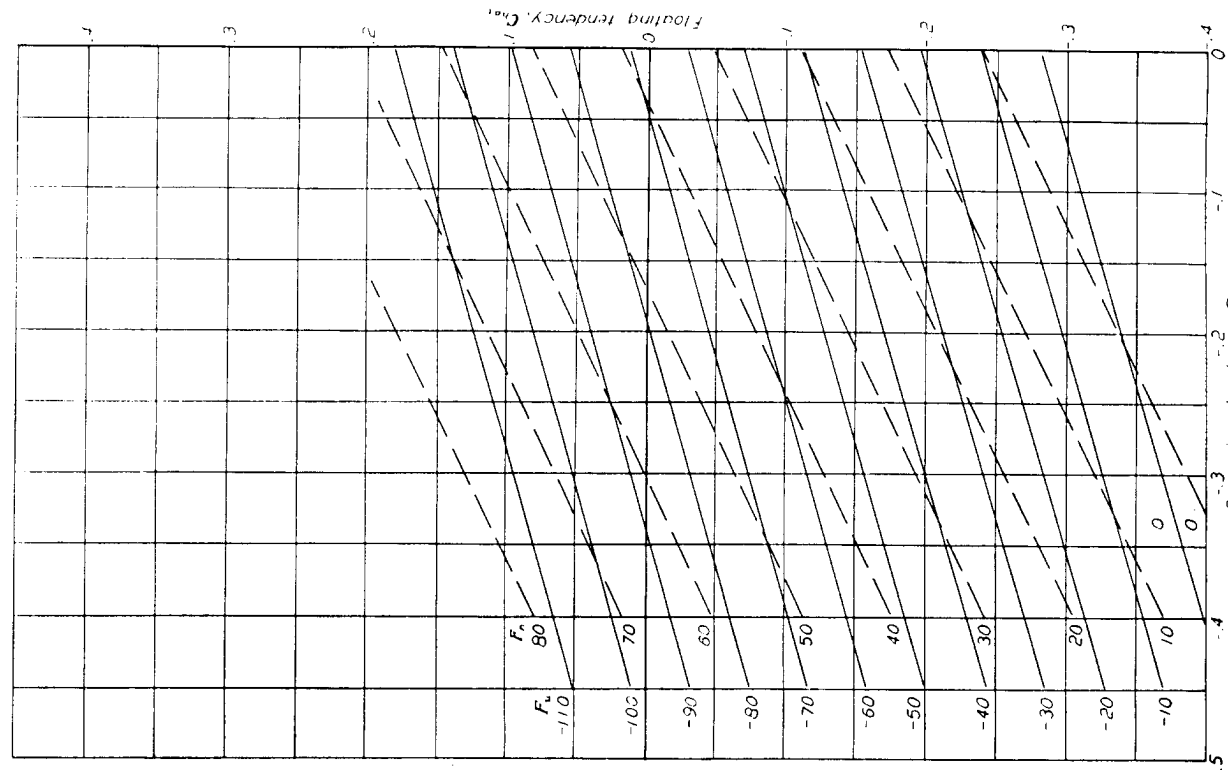

FIGURE 4.—Trim force F_s and pull-up force F_s as functions of hinge-moment parameters. Mass-unbalanced elevator ($h=10$); $\tau_{s,c}=0.05$; $\frac{W}{S_e}=40$ pounds per square foot; $\frac{c}{}=7$ feet; sea level. F_s=stick force in pounds for $\frac{\Delta\Gamma}{V}=1.0$; F_s=stick force in pounds per g normal acceleration.

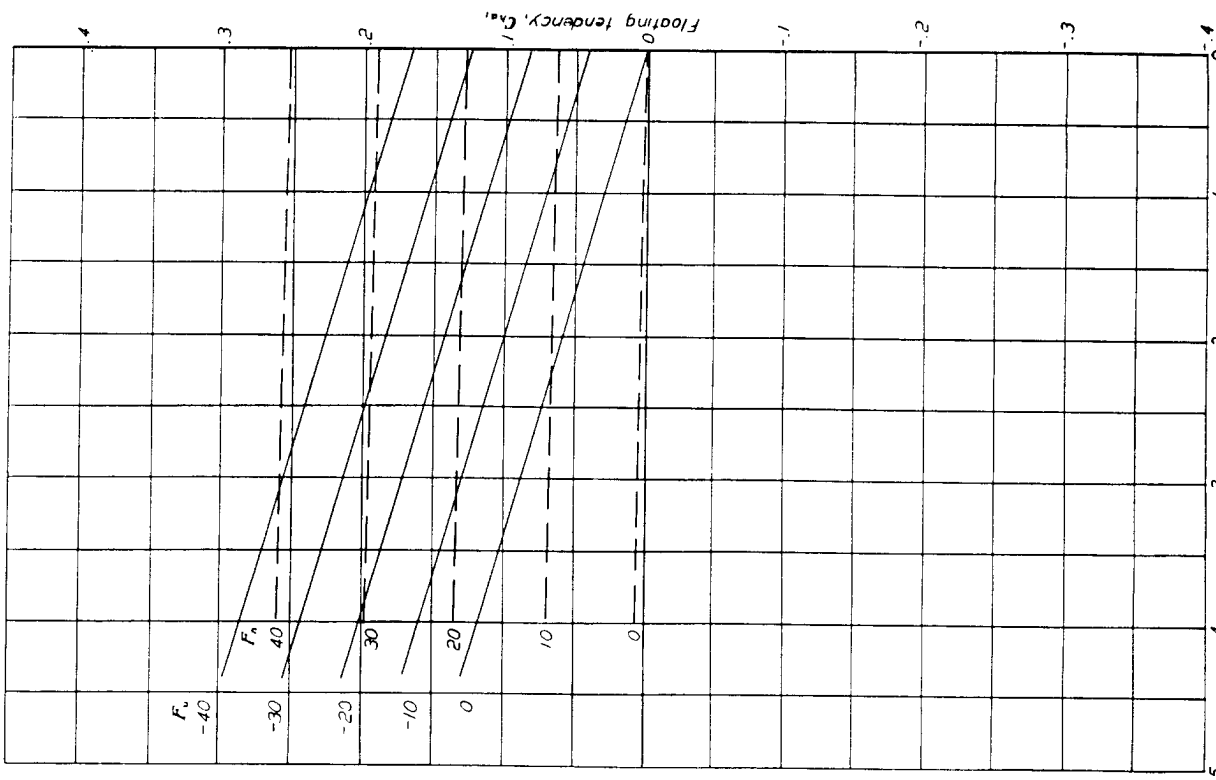

FIGURE 3.—Trim force F_s and pull-up force F_s as functions of hinge-moment parameters. $\tau_{s,c}=-0.05$; $\frac{W}{S_e}=40$ pounds per square foot; $\frac{c}{}=7$ feet; sea level. F_s=stick force in pounds for $\frac{\Delta\Gamma}{V}=1.0$; F_s=stick force in pounds per g normal acceleration.

Increase in altitude will either increase or decrease F_n, depending on the hinge-moment parameters. The solid line in figure 5 is the locus of values of $C_{h_{\alpha_t}}$ and C_{h_δ} for which F_n is independent of altitude. For points to the left of this line, F_n decreases with altitude; for points to the right of this line, F_n increases with altitude. This line is determined by the relation

$$C_{h_{\alpha_t}}=\frac{C_{m_{D\theta}}}{C_{m_\delta} l_h} C_{h_\delta}$$

which, for the case of figure 5, becomes

$$C_{h_{\alpha_t}}=1.50 C_{h_\delta}$$

Another method of increasing the stick-force gradient in level flight F_u consists in applying a constant hinge moment to the elevator by means of a spring or bungee. The effect of the spring on the gradient F_u is due to the derivative C_{h_u} which depends in the same way on the constant hinge moment, whether it is caused by a weight or by a spring. A bungee, which tends to depress the elevator, will therefore increase the stick-force gradient in level flight F_u. The effect of the bungee on the stick-force gradient in accelerated flight F_n will be zero because its action depends solely on changes in forward speed. Its effect on the short-period oscillations will be zero for the same reason.

DYNAMIC STABILITY

NO FRICTION IN CONTROL SYSTEM

The stability of the short-period oscillations without friction is shown in figures 6 to 11, which also show the boundaries for true static stability (divergence boundaries). Figure 6 is an example of a more nearly complete presentation of the stability data than subsequent figures because it shows the variation of damping and period of oscillation with the hinge-moment parameters $C_{h_{\alpha_t}}$ and C_{h_δ} for certain fixed values of the other parameters. The damping, which is proportional to ξ, increases with the magnitude of C_{h_δ}. The period, proportional to $\frac{1}{\eta}$, decreases as $C_{h_{\alpha_t}}$ increases. Another way of presenting this additional stability data is shown in figure 7, which gives the number of cycles the oscillation performs before it damps to half amplitude. It is clear from figure 7 that the oscillation is very well damped unless the restoring tendency is close to zero. In this particular case, only one oscillatory mode exists. Inasmuch as there are only three roots in this case (because i_2 and $i_1=0$), the other root is always real and is of no particular significance in dynamic stability. In cases in which an additional oscillatory mode exists, it is always stable.

The effect of center-of-gravity position on the stability of the short-period oscillations is shown in figure 8. The shift in the dynamic-stability boundary, for the comparatively large shift in center of gravity shown, is practically negligible. Many of the subsequent figures, in which zero static stability is assumed to facilitate computation, therefore are valid for airplanes having a margin of static stability.

The effect of moment of inertia of the elevator control system on the dynamic stability is shown in figure 9, which gives typical values of the moment of inertia. The effect is slightly destabilizing especially for high values of $C_{h_{\alpha_t}}$. The destabilizing effect of the moment of inertia of the elevator is greater than that of the moment of inertia of the control stick. Because the accuracy gained by including moment of inertia is small compared with the saving in labor gained by neglecting it, moment of inertia of the elevator control system was set equal to zero in the subsequent calculation. As a result, the stability equation becomes a cubic and subsequent figures are somewhat unconservative.

The effect of density parameter μ on the dynamic stability is shown in figure 10. Increase of μ has a slight destabilizing effect.

As has been shown, mass unbalance of the elevator control system improves the static stability (fig. 4). The effect on dynamic stability is unfavorable, however, as shown in figure 11. The value of mass unbalance shown corresponds to a bobweight that is located at the airplane center of gravity and requires a balancing pull of 37 pounds on the control stick of a pursuit airplane at sea level. Increasing oscillations occur if the aerodynamic balance is too high (low magnitudes of C_{h_δ}), especially for negative values of C_{h_α}.

The effect of the location of the bobweight is shown in figure 12. Each curve represents a different arrangement of bobweights and all arrangements give the same stick force. The solid line corresponds to a weight at the airplane center of gravity (for practical purposes, at the control stick). The short-dash line corresponds to a weight at the elevator. The long-dash line corresponds to two weights—one at the elevator, which tends to make it noseheavy; the other at the control stick, which gives the elevator a sufficiently powerful tailheavy moment that the resultant stick force is the same as with the single weight. In the particular case represented, the noseheavy moment due to the weight at the elevator is equal to the tailheavy moment due to both weights. Moving the single weight from the control stick to the elevator has a large destabilizing effect. Overbalancing the elevator while the stick force is kept constant has a considerable stabilizing effect. This method of preventing instability has the disadvantage, however, of increasing the total amount of unbalancing weight required. In the case shown, the weight is increased to three times its original size. Another disadvantage is the rearward shift in center of gravity of the whole airplane due to additional weight at the elevator. (See airplane parameters given in "Method of Analysis.") The destabilizing effect of the increased moment of inertia associated with the added weights was found to be very small, especially for negative floating tendency.

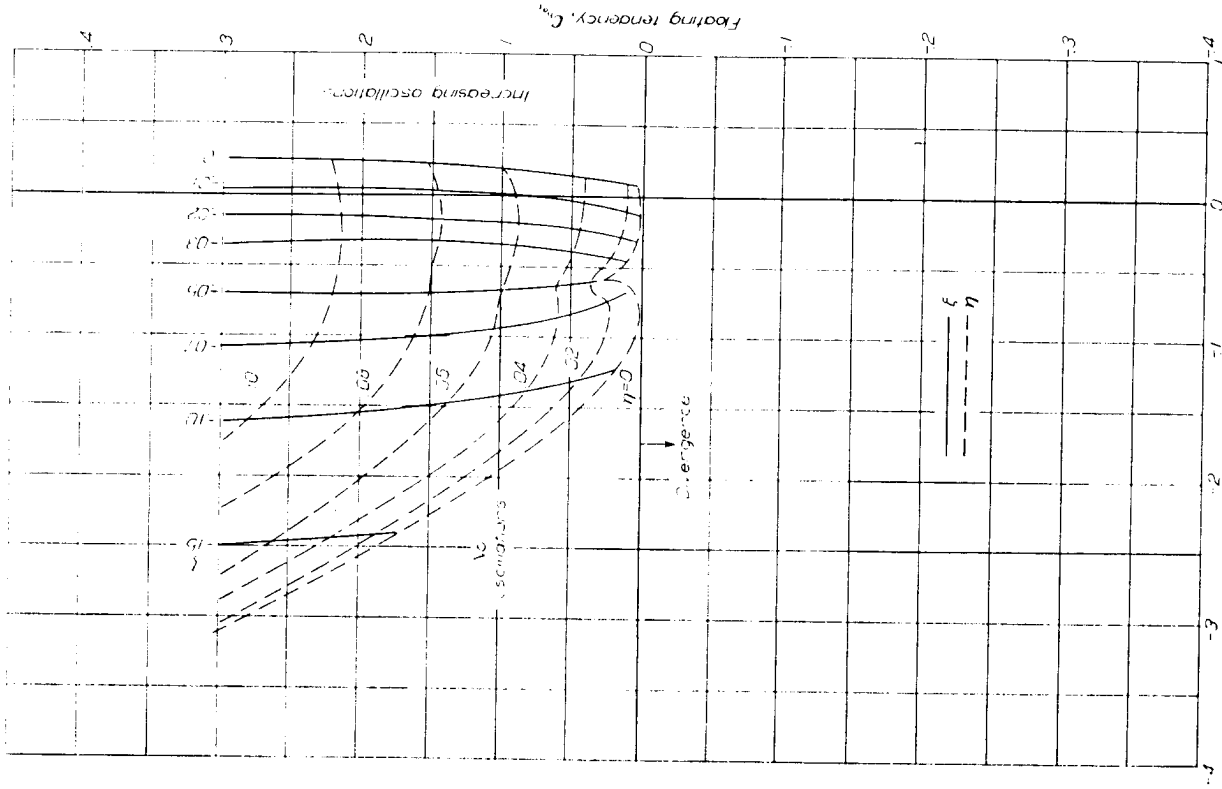

FIGURE 6.—Variation of damping and frequency of control-free longitudinal oscillation with elevator-balance parameters. $I_{a.c.}=0$; $\mu=12.5$; $h=i_t=i_w=0$.

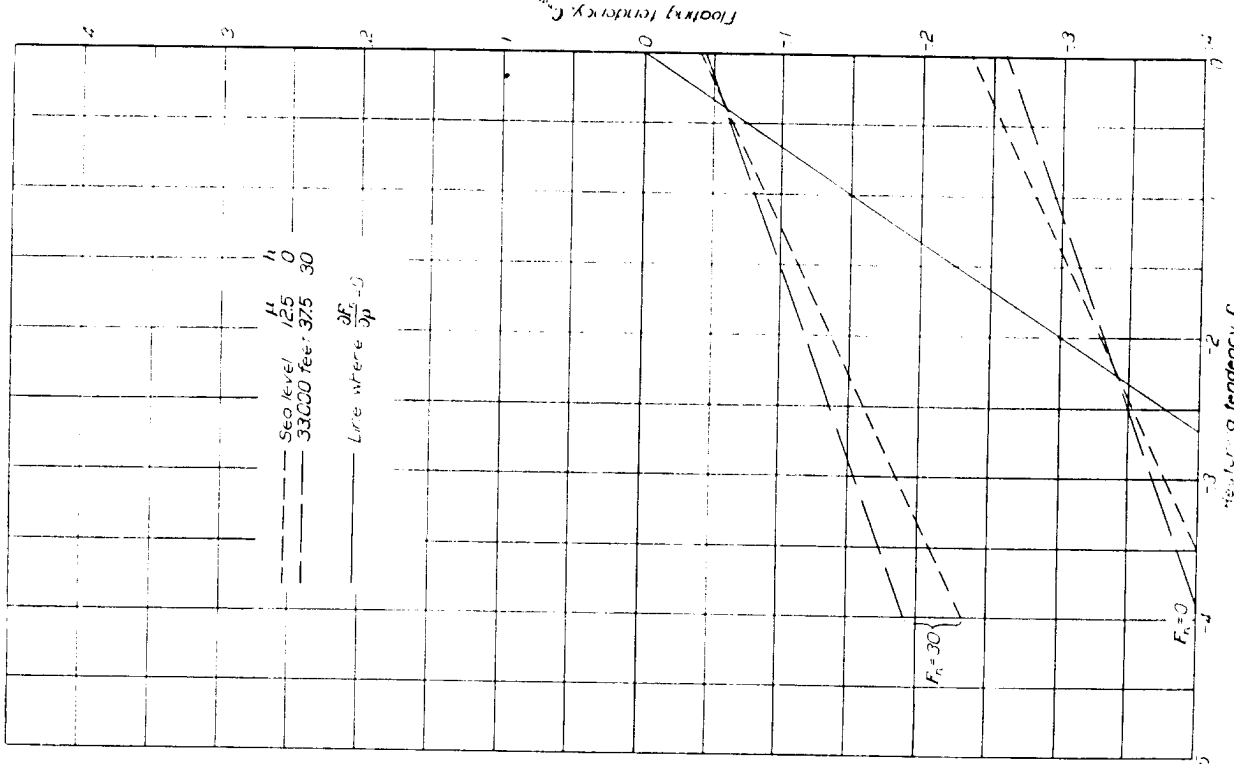

FIGURE 5.—Effect of altitude on values of stick-force gradient. $I_{a.c.}=0.056$; $\frac{W}{S}=40$ pounds per square foot; $c=7$ feet.

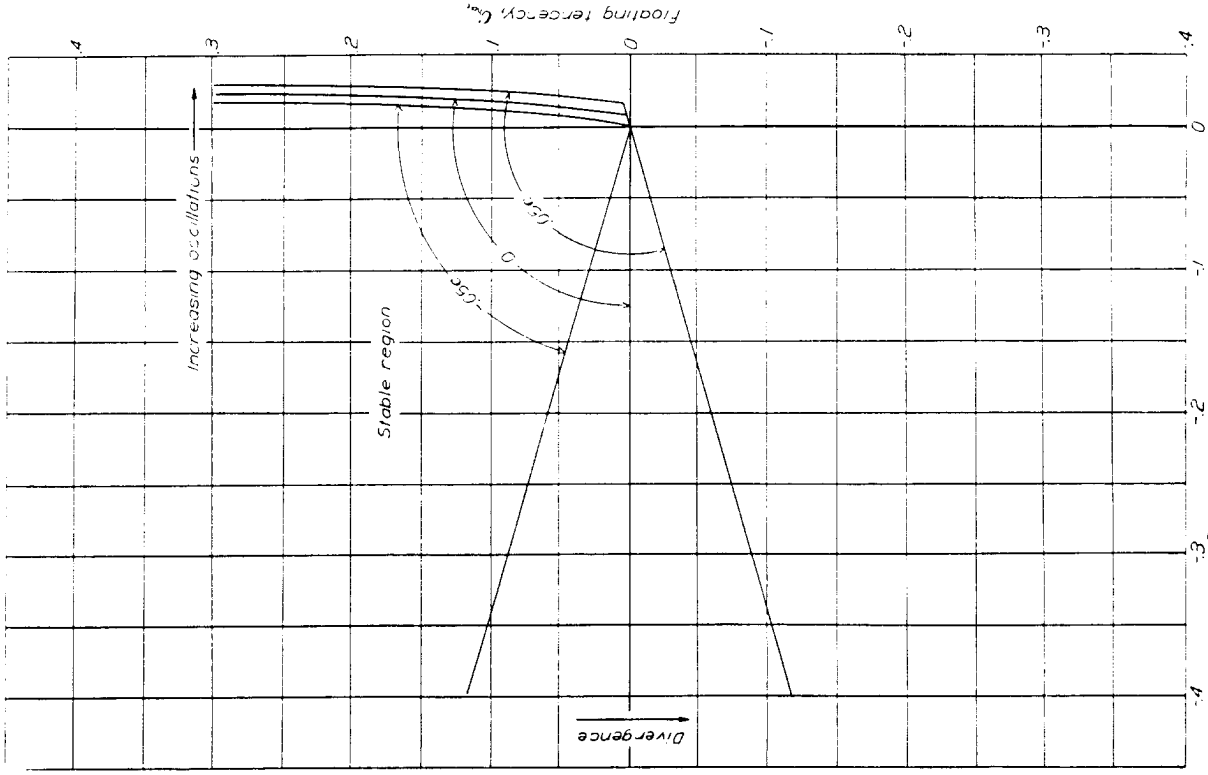

FIGURE 8.—Effect of center-of-gravity location on stability boundaries. $\mu=12.5$.

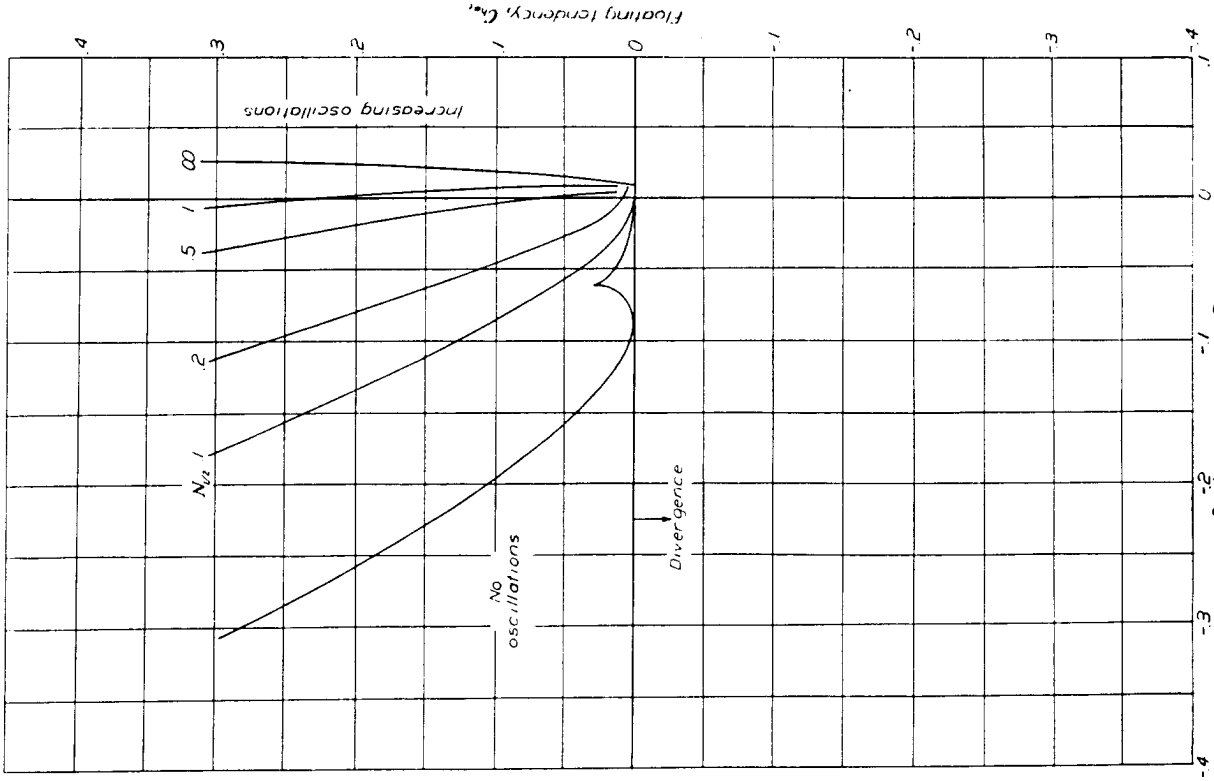

FIGURE 7.—Number of cycles to damp to half amplitude $N_{1/2}$ against hinge-moment parameters. $I_{\alpha_i}=0$; $\mu=12.5$; $h=i_t=i_b=0$.

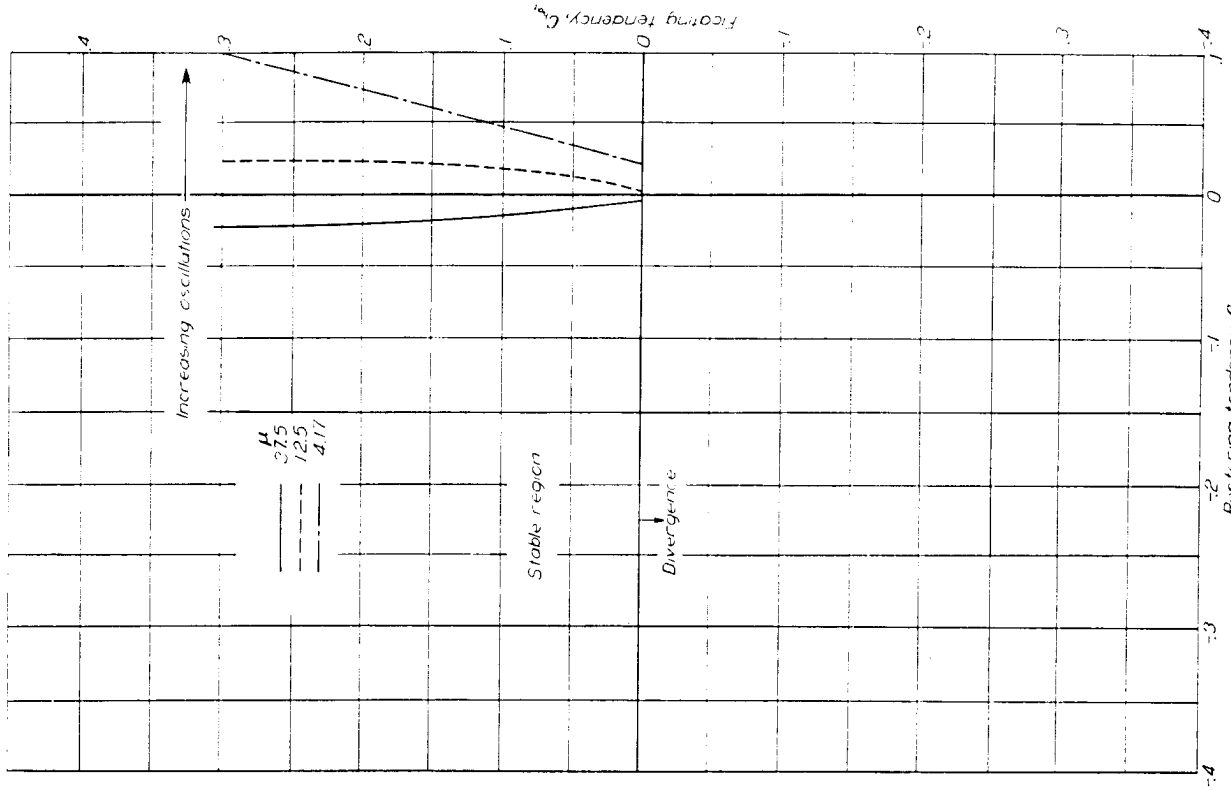

FIGURE 10.—Variation of stability boundaries with density parameter.

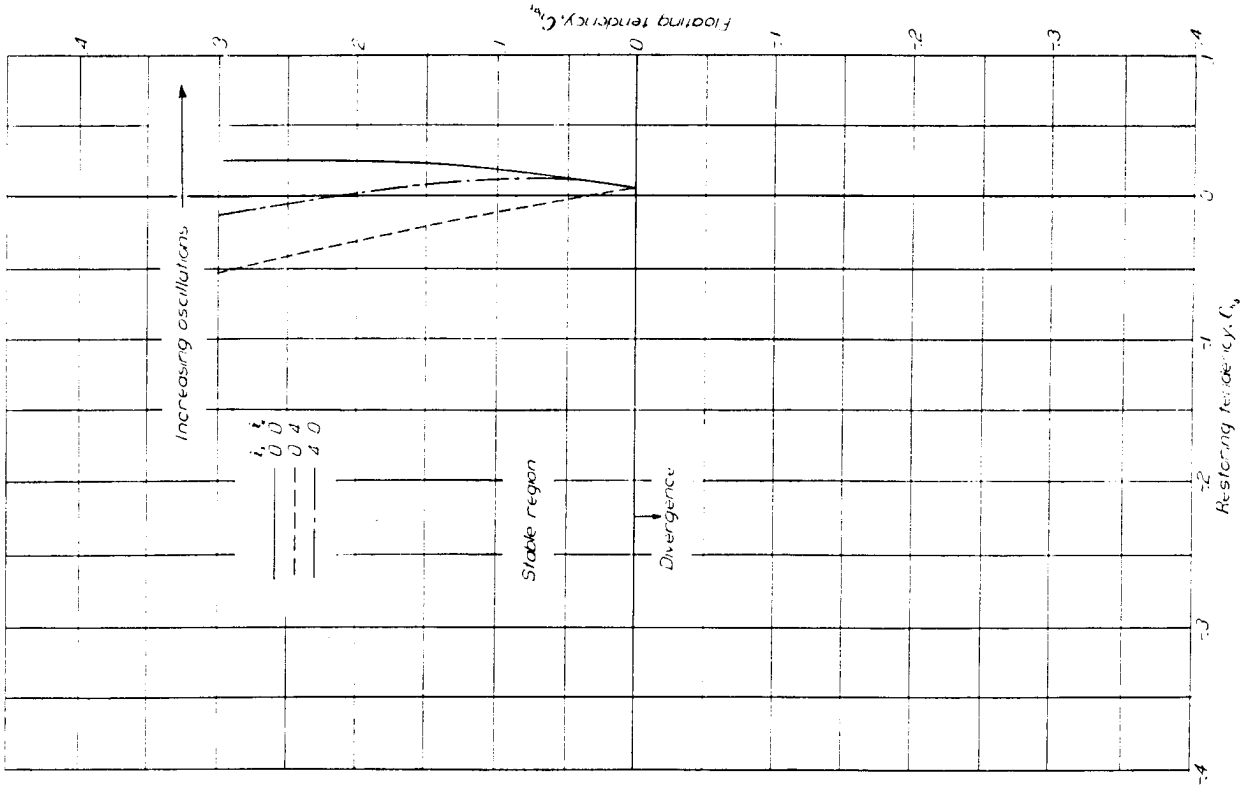

FIGURE 9.—Effect of elevator control-system moment of inertia on the boundary for increasing oscillations. $\mu = 12.5$.

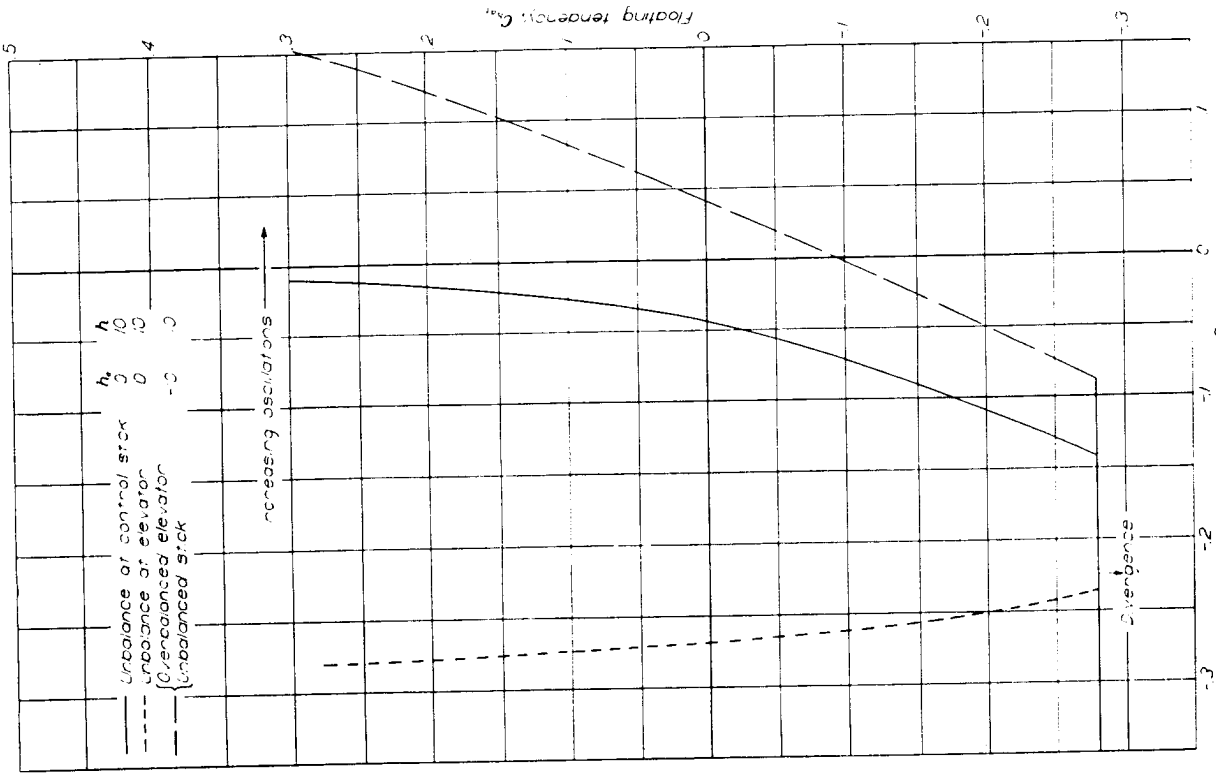

FIGURE 12.—Effect of location of mass unbalance of the elevator control system on the stability boundaries. $\mu = 12.5$; $i_A = 0$; $i_t = 0$.

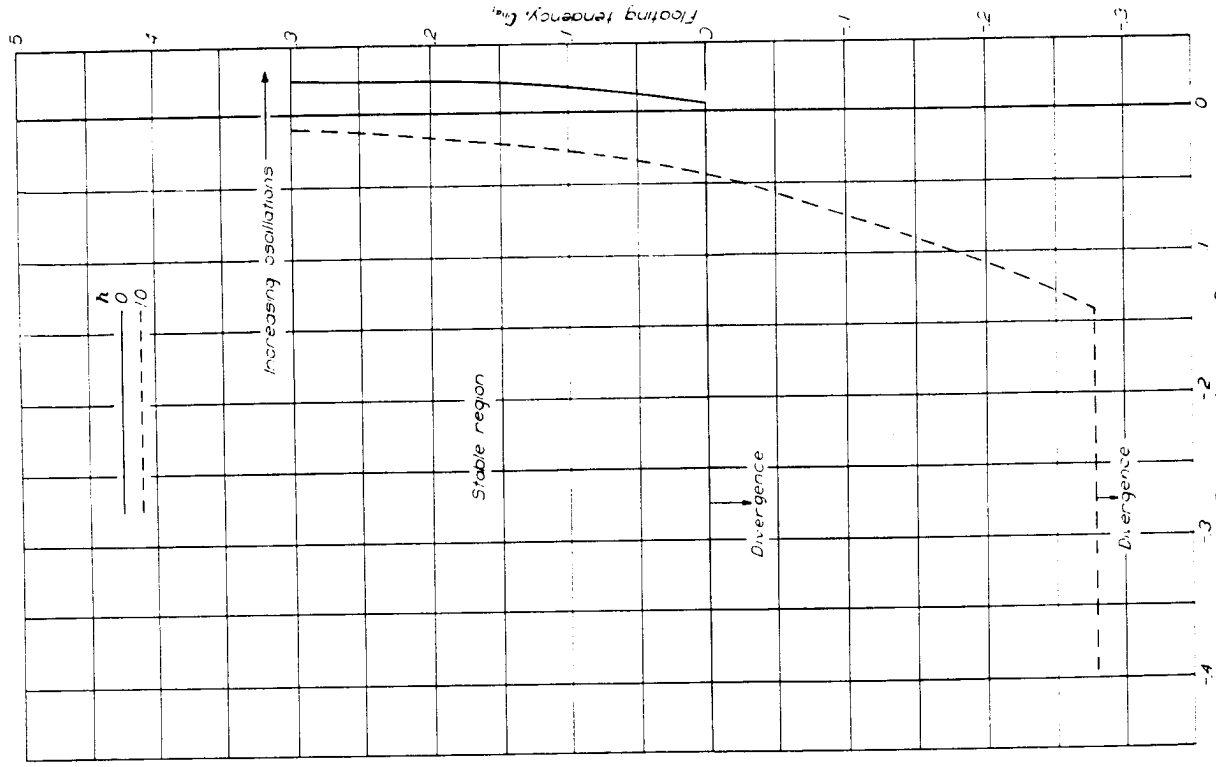

FIGURE 11.—Effect of mass unbalance of the elevator control system on the stability boundaries. $\mu = 12.5$

EFFECT OF VISCOUS FRICTION IN CONTROL SYSTEM

In the preceding section, a constant value of the elevator-damping parameter $C_{h_{D\delta}}$ was assumed. This value was due only to aerodynamic damping. The effects of viscous friction in the elevator control system are obtained by considering $C_{h_{D\delta}}$ as an additional variable. This variable can be introduced, as in the preceding section, by showing a series of boundaries in the $C_{h_{\alpha_t}}C_{h_\delta}$ plane for various values of $C_{h_{D\delta}}$. The general nature of the effect of friction is shown first, however, by presenting boundaries in the $C_{h_\delta}C_{h_{D\delta}}$ plane with $C_{h_{\alpha_t}}$ constant and some other parameter varied. This method of presenting stability boundaries makes it easier to show the effects of other parameters such as airplane center-of-gravity position and density when friction is introduced.

The effect of viscous friction on the dynamic stability, for various conditions, is shown in figures 13 and 14 for $\mu=12.5$ and $\mu=37.5$, respectively. Figures 13(a) and 14(a) refer to the mass-balanced elevator control system; figures 13(b) and 14(b) refer to the tailheavy elevator control system considered in the preceding section. It is shown that, if the airplane center of gravity is ahead of a certain point,[1] the instability caused by the unbalanced elevator can be removed by adding viscous friction to the control system. This critical center-of-gravity position is behind the aerodynamic center, and its distance from the aerodynamic center decreases as the density parameter μ increases. When the center of gravity is behind this critical position, viscous friction has a destabilizing effect. These opposite effects of viscous friction are shown in the $C_{h_{\alpha_t}}C_{h_\delta}$ plane in figures 15 and 16. When the center of gravity is slightly ahead of this critical position, the effect of viscous friction depends on its magnitude and also on the value of C_{h_δ}. The addition of a small amount of viscous friction is destabilizing but larger amounts are stabilizing. If the aerodynamic balance is sufficiently high ($C_{h_\delta}\approx 0$) and the viscous friction lies in a certain range, increasing oscillations will occur. In figure 14(b), for example, if $x_{a.c.}=-0.01c$ and $C_{h_\delta}=-0.05$, the oscillations will be unstable when the elevator-damping parameter is in the range from -2.5 to -76. If C_{h_δ} is more negative than -0.086, no amount of elevator damping can cause increasing oscillations. As the center of gravity moves forward, the destabilizing effect of elevator damping becomes less and finally disappears.

The effect of the density parameter μ can be seen by comparing figures 13 and 14. The critical center-of-gravity position approaches the aerodynamic center as μ increases. When $\mu=12.5$, elevator damping always has a stabilizing effect provided $x_{a.c.}$ is positive. When $\mu=37.5$, elevator damping may be destabilizing over a small range of $C_{h_{D\delta}}$ and C_{h_δ} even when $x_{a.c.}$ is positive ($0.05c$).

When the center of gravity is slightly ahead of the aforementioned critical position (which is behind the aerodynamic center), the conditions under which elevator damping may cause dynamic instability may be advantageously represented in the $C_{h_{\alpha_t}}C_{h_\delta}$ plane. If a series of stability boundaries are drawn in that plane for various values of elevator damping, they will all be confined to a region bounded by a line that will be called the boundary of complete damping. An illustration of two methods of constructing this boundary is given in figure 17. If a series of boundaries in the $C_{h_{\alpha_t}}C_{h_\delta}$ plane are drawn for various values of the damping, the common tangent of all these curves is the boundary for complete damping. This boundary can also be drawn by plotting the minimum values of C_{h_δ} obtained from plots of the type shown in figures 13 and 14 against corresponding values of $C_{h_{\alpha_t}}$. The region in the $C_{h_{\alpha_t}}C_{h_\delta}$ plane between the boundaries for complete damping and increasing oscillations is the region where the addition of viscous friction to the elevator control system may cause dynamic instability.

That a boundary for complete damping cannot be shown for $\mu=12.5$ if the airplane is statically neutral or stable ($x_{a.c.}$ is zero or positive) may be seen from figure 13. It is possible however, to show a boundary for complete damping under these conditions for $\mu=37.5$. Figure 18 shows these boundaries for $x_{a.c.}=0$ and for the critical value $x_{a.c.}=-0.017c$, for both a mass-balanced elevator and a mass-unbalanced elevator. The boundaries for increasing oscillations and divergence are also shown. For the case of the mass-balanced elevator ($h=0$), the boundary for complete damping is a straight line through the origin and therefore corresponds to a fixed ratio of the floating and restoring tendencies, or floating ratio. Elevator mass unbalance decreases the region of complete damping.

EFFECT OF SOLID FRICTION IN ELEVATOR CONTROL SYSTEM

The boundary for complete damping has an important bearing on the effect of solid friction on dynamic stability. In order to calculate this effect, the solid friction is replaced by an equivalent viscous friction that would dissipate energy at the same rate. This condition gives an equivalent

$$C_{h_{D\delta}}=\frac{4}{\pi}\frac{C_{h_f}}{\eta\bar{\delta}} \tag{4}$$

for a sinusoidal motion of the elevator with amplitude $\bar{\delta}$ and angular frequency η.

[1] Since this report was written, this point has been found to be where $\frac{d\delta}{dn}=0$, sometimes called the stick-fixed maneuver point.

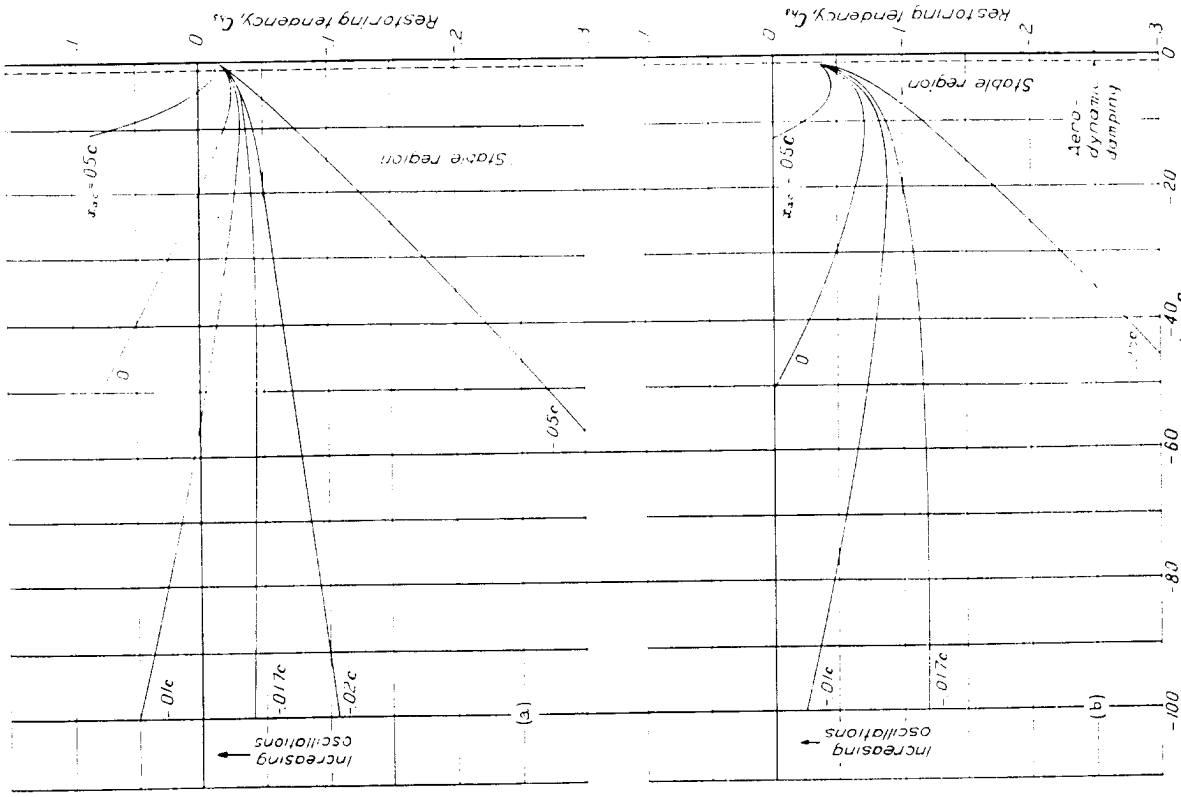

FIGURE 14.—Effect of elevator damping on the boundary for increasing oscillations for various center-of-gravity locations and elevator-mass-balance conditions. $C_{h_{\alpha_1}}=0.1$; $\mu=47.5$.
(a) $h=0$.
(b) $h=10$.

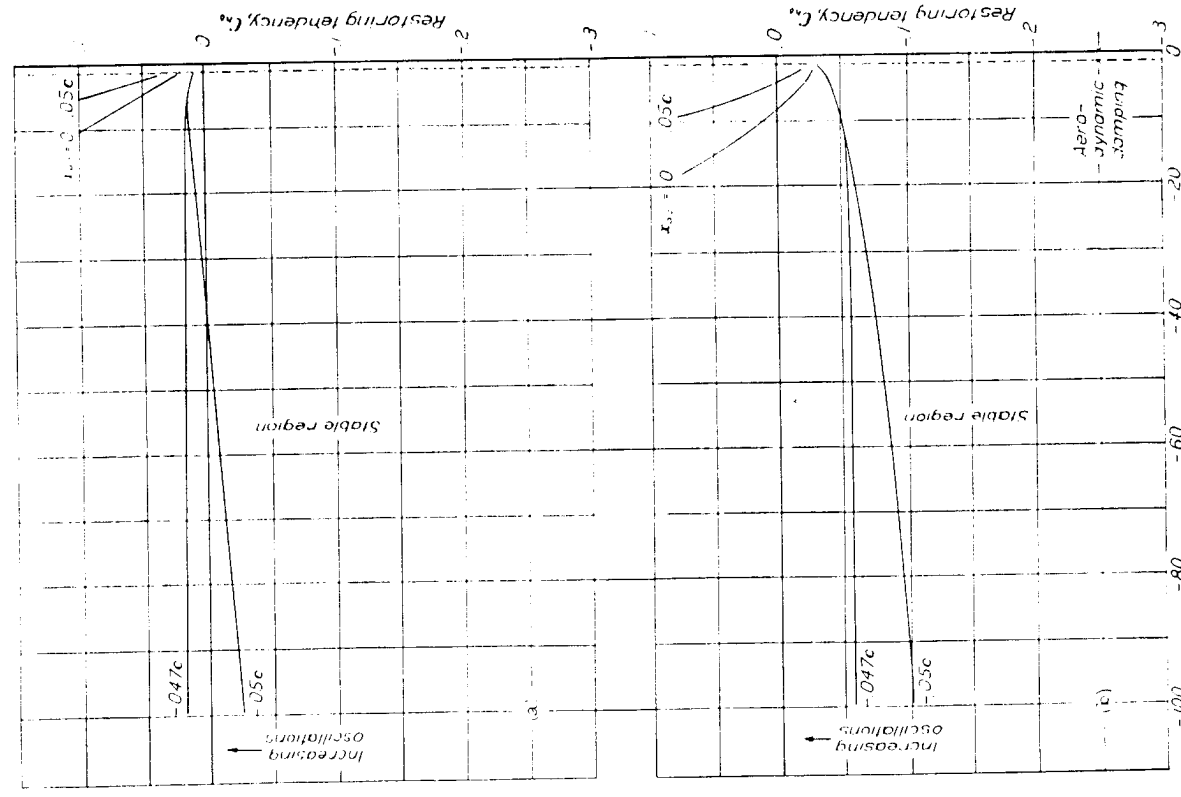

FIGURE 13.—Effect of elevator damping on the boundary for increasing oscillations for various center-of-gravity locations and elevator-mass-balance conditions. $C_{h_{\alpha_1}}=0.1$; $\mu=12.5$.
(a) $h=0$.
(b) $h=10$.

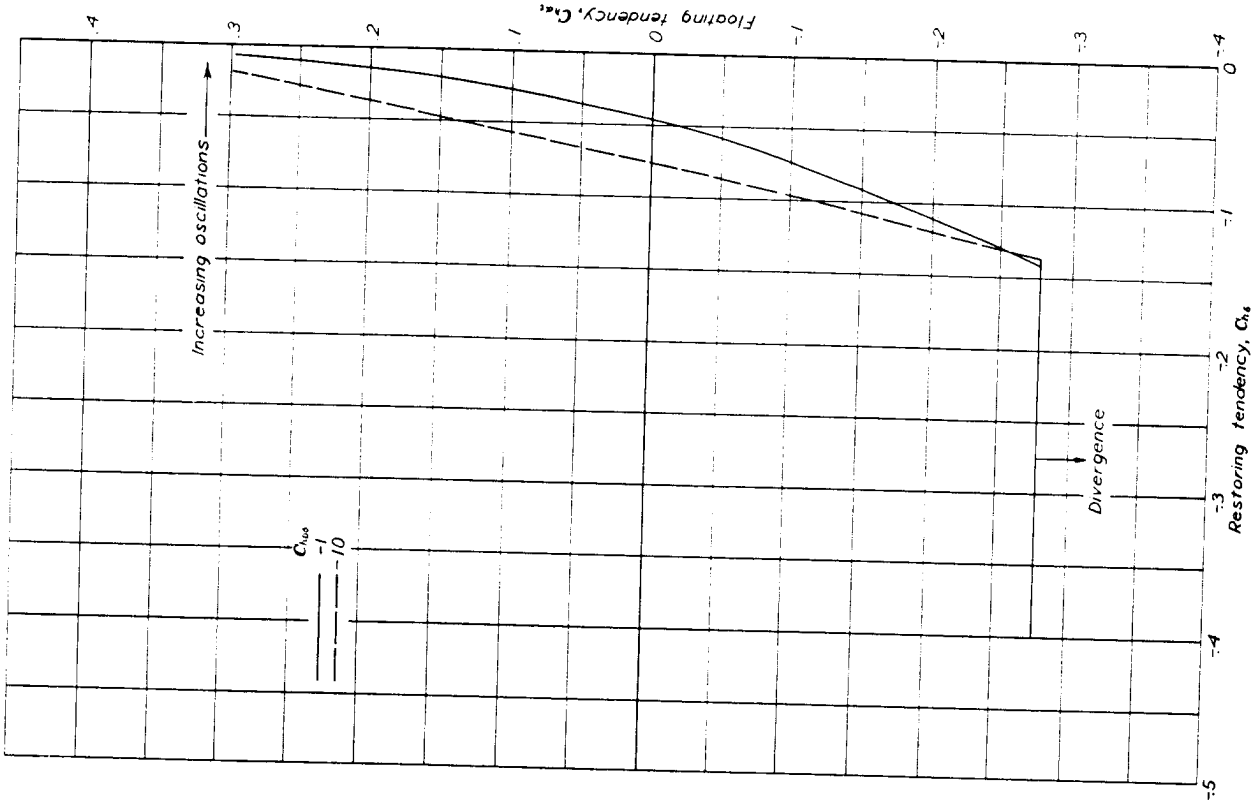

FIGURE 16.—Illustration of destabilizing effect of elevator damping (viscous friction). $\tau_{e,e_1} = -0.05$; $\mu = 12.5$; $h = 10$.

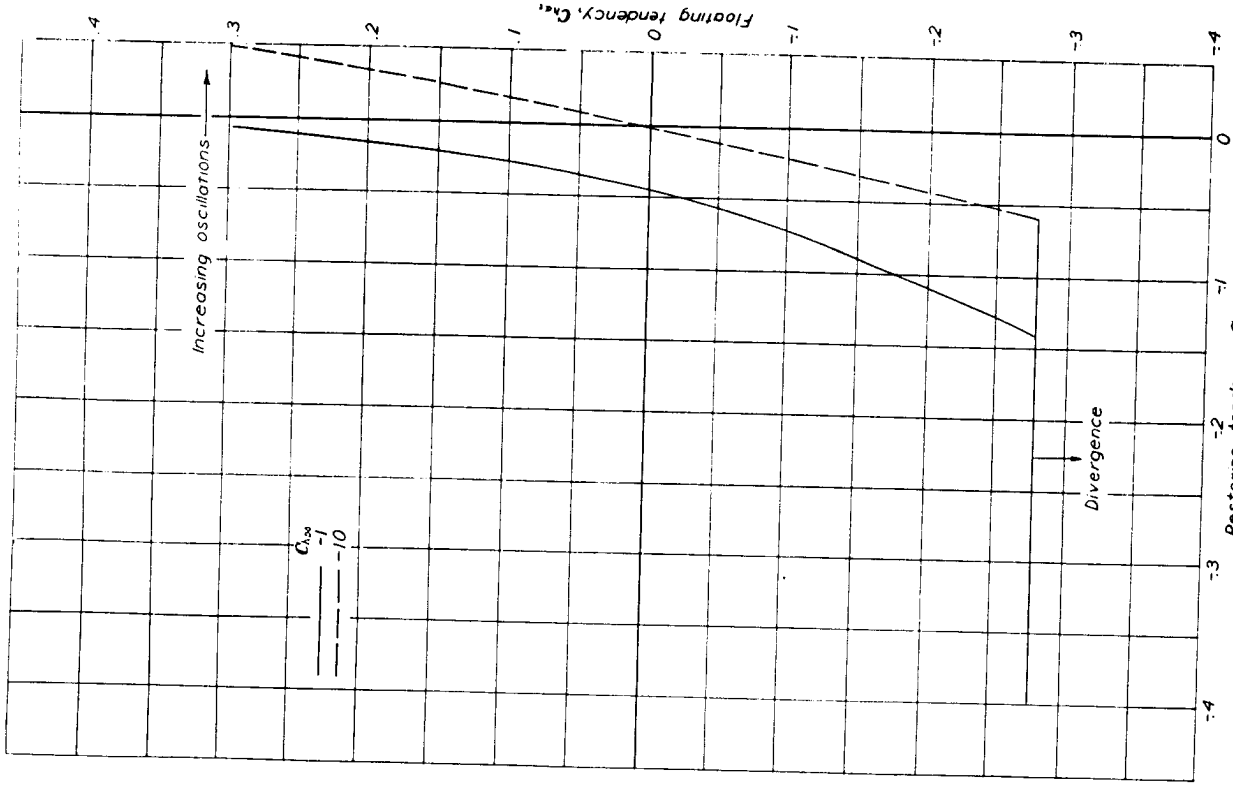

FIGURE 15.—Illustration of stabilizing effect of elevator damping (viscous friction). $\tau_{e,e_1} = 0$; $\mu = 12.5$; $h = 10$.

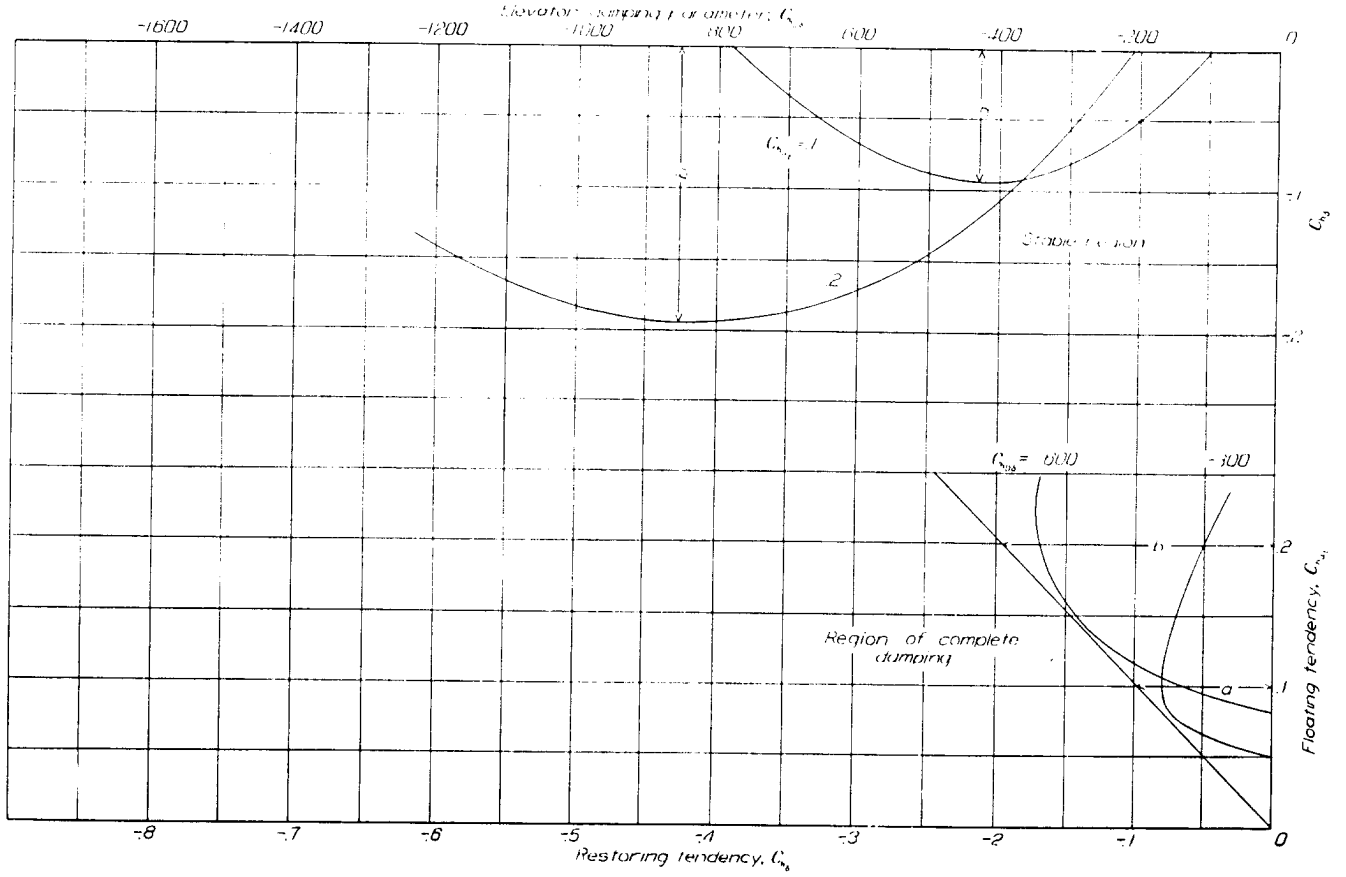

FIGURE 17.—Method of constructing boundary for complete damping.

It can be shown that if viscous friction is destabilizing, as in figures 16 to 18, solid friction may lead to steady oscillations having an amplitude proportional to the amount of friction. Suppose an oscillation is started with amplitude and frequency which result in an equivalent $C_{h_{D\delta}}$ that would cause increasing oscillations. Let this condition be represented by point 2 in figure 19. The amplitude of the oscillations would then increase until the equivalent $C_{h_{D\delta}}$ decreased to the value that would result in neutrally damped oscillations, represented by point 3 in figure 19. If the initial amplitude is so low that the equivalent viscous friction is in the stable region, as shown by point 1, the oscillations will die out completely. If the initial amplitude is so high that the oscillations are stable, represented by point 4, the amplitude will decrease until it reaches a constant value, when the equivalent $C_{h_{D\delta}}$ is again represented by point 3. The value of $C_{h_{D\delta}}$ at point 3 then determines the amplitude of the steady oscillations. By solving formula (4) for $\bar{\delta}$, the amplitude of the steady oscillation is obtained as

$$\bar{\delta}=\frac{4}{\pi}\frac{C_{h_f}}{\eta C_{h_{D\delta}}}$$

where η and $C_{h_{D\delta}}$ are the values at point 3. This formula shows that the amplitude is proportional to the amount of solid friction.

The foregoing analysis shows that the region in the $C_{h_{\alpha_t}} C_{h_\delta}$ plane between the boundary for increasing oscillations and the boundary for complete damping is the region where steady oscillations may occur because of the influence of solid friction in the control system. All the remarks in the preceding section concerning the boundary for complete damping with viscous friction consequently apply to the boundary for steady oscillations with solid friction, inasmuch as these two boundaries are the same, within the limits of the assumptions involved in the use of the concept of equivalent viscous friction. Steady oscillations due to solid friction will not occur on a statically neutral or stable airplane, for instance, unless μ is very large (corresponds to a high altitude). Even in that case, the possibility of steady oscillations exists only for a comparatively small range of floating ratios. If the airplane is statically unstable by a sufficient amount, however, steady oscillation may exist over the entire range of floating ratio.

Some calculations of the amplitude of the steady oscillations, expressed in terms of normal acceleration per unit frictional force as felt at the control stick, were made by the

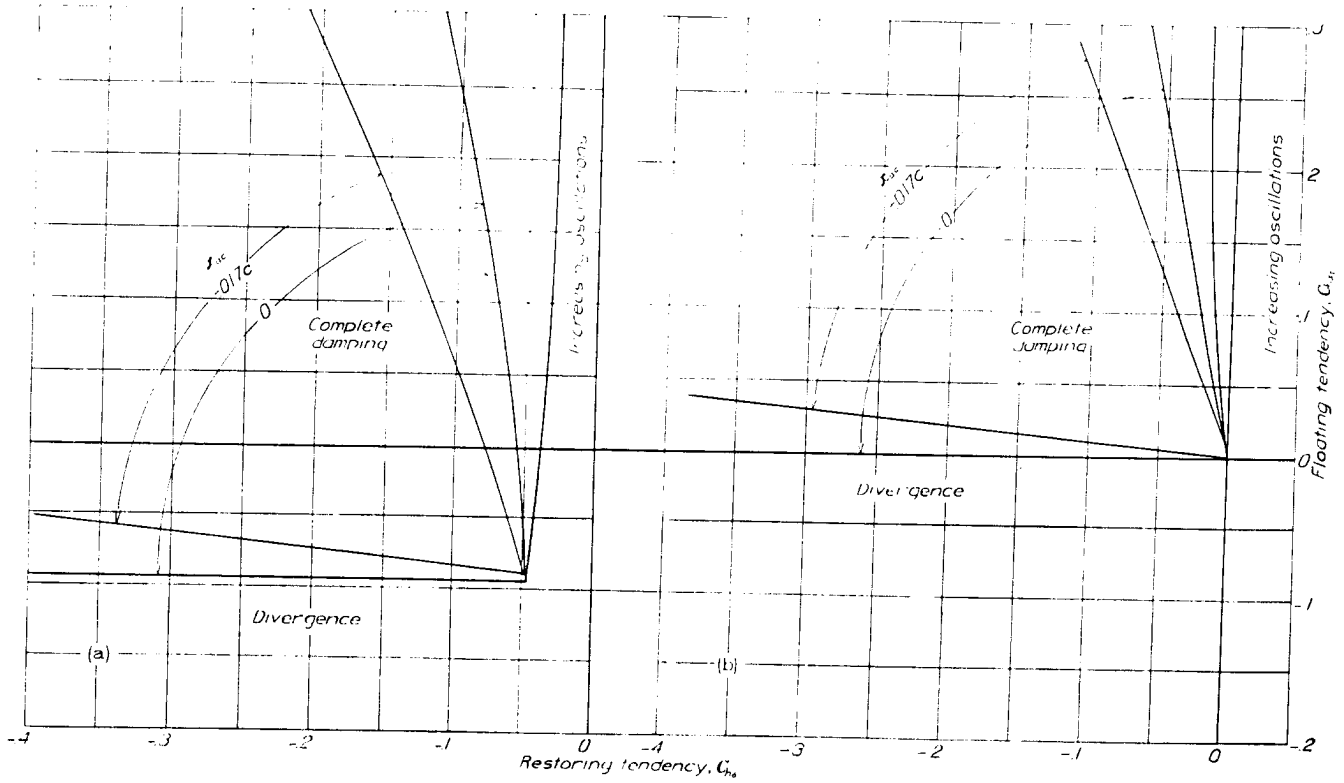

(a) $h=10$.
(b) $h=0$.

FIGURE 18.—Boundaries for complete damping, increasing oscillations, and divergence. $\mu=37.5$.

method of appendix B. The results are presented in figure 20, which shows lines of constant amplitude in the $C_{h_{\alpha_t}} C_{h_\delta}$ plane for an airplane with the center of gravity at the critical position referred to in the preceding section. Steady oscillations will therefor occur throughout the entire region where stability exists in the absence of friction. The amplitude is smallest for high values of $C_{h_{\alpha_t}}$ combined with high values of C_{h_δ}.

CONCLUDING REMARKS

The stick-free static stability of a conventional airplane may be improved by making the elevator floating tendency more positive or by mass-unbalancing the elevator control system to make the elevator tailheavy. Increasing the restoring tendency also has a favorable effect provided the airplane is stable with stick fixed. If the restoring tendency is zero, the stick-free static stability is independent of airplane center-of-gravity position.

The dynamic stability with frictionless controls depends chiefly on the restoring tendency C_{h_δ} and on the mass balance of the elevator control system. If the elevator control system is mass unbalanced (elevator made tailheavy) by an offset weight at the control stick and if the restoring tendency is too low, increasing short-period oscillations may result. This condition can be remedied by the use of two additional weights—one at the elevator making it noseheavy, the other at the control stick making the elevator sufficiently tailheavy that the combined effect gives the elevator the desired amount of tailheaviness.

The addition of viscous friction to the control system will prevent dynamic instability provided the airplane center of gravity is forward of a critical position which is behind the aerodynamic center and approaches it as the value of the density parameter μ increases. If the airplane center of gravity is behind this critical position, viscous friction will have a destabilizing effect, no matter what the hinge-moment parameters are. If the center of gravity is slightly ahead of the critical position, viscous friction may be destabilizing for a limited range of values of viscous friction and the hinge-moment parameters. A low restoring tendency and a high positive floating tendency will tend to cause this dynamic instability. When μ is very large (high altitude), this condition of steady oscillations can occur even if the center of gravity is ahead of the aerodynamic center.

The presence of solid friction in the control system may cause short-period steady oscillations under the conditions for which viscous friction is destabilizing. The amplitude of the oscillations is proportional to the amount of friction present.

LANGLEY MEMORIAL AERONAUTICAL LABORATORY,
NATIONAL ADVISORY COMMITTEE FOR AERONAUTICS,
LANGLEY FIELD, VA., *December 23, 1943.*

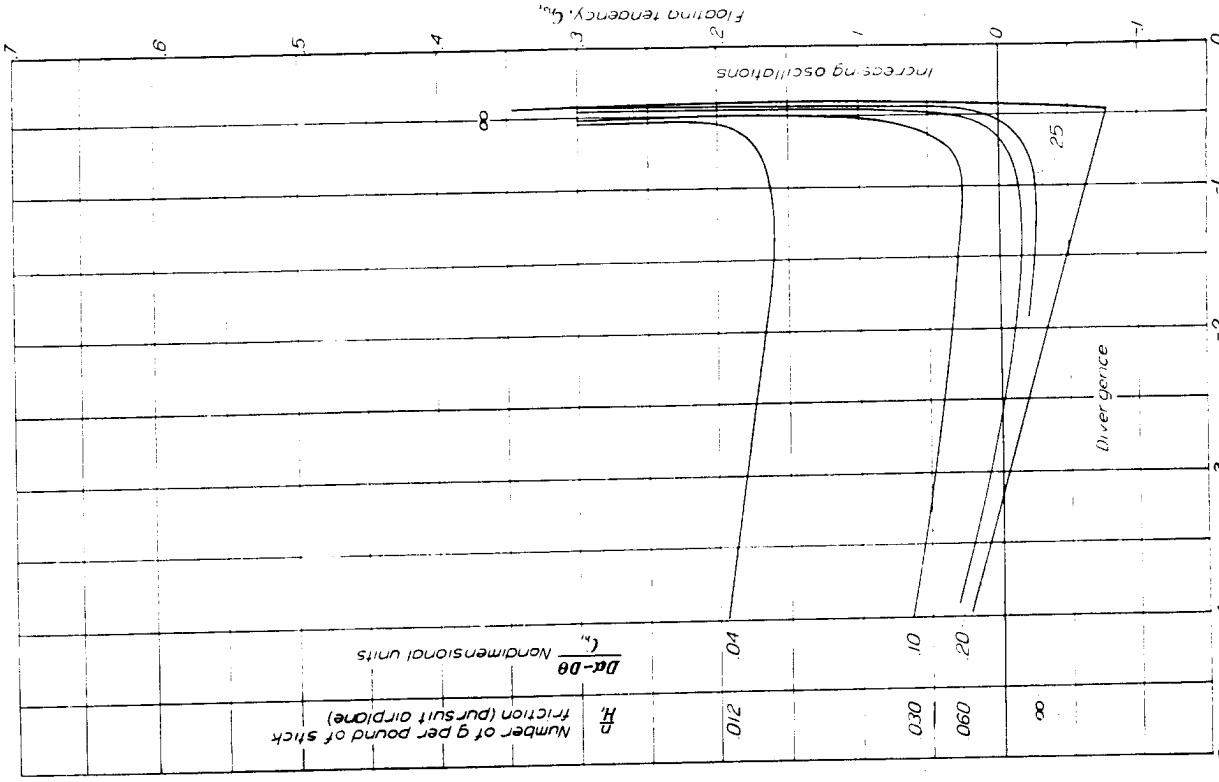

FIGURE 19.—Effect of solid friction in building up steady oscillations.

FIGURE 20.—Variation of maximum normal acceleration in the steady oscillation with elevator hinge-moment parameters. $I_{Y'}=0.05$; $\mu=37.5$; $h=10$; $i_t=2$; $i_e=0$.

APPENDIX A

EVALUATION OF STABILITY DERIVATIVES

Derivative C_{h_u}.—The total hinge moment acting on the elevator may be expressed as

$$H=(C_{h_\alpha}\alpha+C_{h_\delta}\delta_e)\frac{1}{2}\rho V^2 S_e c_e+H_0 g$$

$$H_V=\frac{\partial H}{\partial V}=(C_{h_\alpha}\alpha+C_{h_\delta}\delta_e)\rho V S_e c_e$$

At trim $H=0$, therefore,

$$C_{h_\alpha}\alpha+C_{h_\delta}\delta_e=-\frac{H_0 g}{\frac{1}{2}\rho V^2 S_e c_e}$$

$$H_V=-\frac{H_0}{\frac{1}{2}\rho V^2 S_e c_e}\rho V S_e c_e=-\frac{2H_0 g}{V}$$

$$C_{h_u}=\frac{\partial H\Big/\frac{1}{2}\rho V^2 S_e c_e}{\partial V/V}=\frac{2H_V}{\rho V S_e c_e}=-\frac{4H_0 g}{\rho V^2 S_e c_e}$$

If $H_0=\frac{h\rho S_e c_e c}{4}$,

$$C_{h_u}=-\frac{hcg}{V^2}$$

Using $\frac{1}{2}\rho V^2 C_L S_w=mg$ gives

$$C_{h_u}=-\frac{hcg\rho C_L S_w}{2mg}=-\frac{hC_L}{2A_w\mu}$$

Derivative C_{m_α}.—The parameter C_{m_α} may be obtained from wind-tunnel measurements or, if the position of the aerodynamic center of the complete airplane is known, may be calculated by the formula

$$C_{m_\alpha}=-C_{L_\alpha}x_{a.c.}$$

Derivatives $C_{m_{D\alpha}}$ and $C_{m_{D^2\alpha}}$.—The derivatives $C_{m_{D\alpha}}$ and $C_{m_{D^2\alpha}}$ arise because of the lag between the change in angle of attack at the wing and the corresponding downwash at the tail. It is assumed that the downwash at any instant t depends on the angle of attack at the instant $t-\frac{L_h}{V}$, the difference being the time required for the air to move from the wing to the tail. If $\alpha=f(t)$, this relation may be expressed as

$$\epsilon=\epsilon_\alpha f(t-\Delta t)$$

where

$$\Delta t=\frac{L_h}{V}$$

Now,

$$f(t-\Delta t)=f(t)-\Delta t f'(t)+\frac{(\Delta t)^2}{2!}f''(t)-\ \ldots$$

Hence,

$$\epsilon=\epsilon_\alpha\left[\alpha-\Delta t\,\dot{\alpha}+\frac{(\Delta t)^2}{2}\ddot{\alpha}-\ \ldots\right]$$

or, because $\dot{\alpha}=\frac{2V}{C}D\alpha$ and $\ddot{\alpha}=\frac{4V^2}{C^2}D^2\alpha$,

$$\epsilon=\epsilon_\alpha\left(\alpha-l_h D\alpha+\frac{l_h^2}{2!}D^2\alpha-\ \ldots\right)$$

and, because $\alpha_t=\alpha-\epsilon$,

$$\alpha_t=\alpha-\epsilon_\alpha\left(\alpha-l_h D\alpha+\frac{l_h^2}{2!}D^2\alpha-\ \ldots\right)$$

and

$$\alpha_t=\alpha(1-\epsilon_\alpha)+\epsilon_\alpha l_h D\alpha-\epsilon_\alpha\frac{l_h^2}{2}D^2\alpha+\ \ldots$$

The part of the pitching-moment coefficient contributed by the tail is

$$C_m=-C_{L_{t_{\alpha_t}}}\frac{l_h}{2}\frac{S_t}{S_w}\alpha_t$$

$$=-C_{L_{t_{\alpha_t}}}\frac{l_h}{2}\frac{S_t}{S_w}\left[\alpha(1-\epsilon_\alpha)+\epsilon_\alpha l_h D\alpha-\epsilon_\alpha\frac{l_h^2}{2}D^2\alpha\ \ldots\right]$$

The lag effectively introduces derivatives $C_{m_{D\alpha}}, C_{m_{D^2\alpha}}, \ldots$. The first two of these derivatives are

$$C_{m_{D\alpha}}=-C_{L_{t_{\alpha_t}}}\frac{l_h^2}{2}\frac{S_t}{S_w}\epsilon_\alpha$$

and

$$C_{m_{D^2\alpha}}=C_{L_{t_{\alpha_t}}}\frac{l_h^3}{4}\frac{S_t}{S_w}\epsilon_\alpha$$

Derivatives C_{h_α}, $C_{h_{D\alpha}}$, and $C_{h_{D^2\alpha}}$.—The derivatives C_{h_α}, $C_{h_{D\alpha}}$, and $C_{h_{D^2\alpha}}$ may be obtained from

$$\begin{aligned} C_h &= C_{h_{\alpha_t}}\alpha_t \\ &= C_{h_{\alpha_t}}(1-\epsilon_\alpha)\alpha + C_{h_{\alpha_t}}\epsilon_\alpha l_h D\alpha - C_{h_{\alpha_t}}\epsilon_\alpha \frac{l_h^2}{2} D^2\alpha \end{aligned}$$

which gives

$$C_{h_\alpha} = C_{h_{\alpha_t}}(1-\epsilon_\alpha)$$

$$C_{h_{D\alpha}} = C_{h_{\alpha_t}}\epsilon_\alpha l_h$$

$$C_{h_{D^2\alpha}} = -C_{h_{\alpha_t}}\epsilon_\alpha \frac{l_h^2}{2}$$

Derivative $C_{m_{D\theta}}$.—The pitching moment due to pitching is made up of parts due to propeller, wing, fuselage, and horizontal tail. The contribution of the tail is by far the largest and can easily be calculated.

If the airplane is rotating with angular velocity $\dot{\theta}$, the increase in angle of attack at the tail is $L_h \frac{\dot{\theta}}{V}$, which results in an increased lift on the tail given (in coefficient form) by

$$C_{L_t} = C_{L_{t_{\alpha_t}}} L_h \frac{\dot{\theta}}{V}$$

The resultant pitching-moment coefficient is

$$C_m = -C_{L_t}\frac{L_h}{c}\frac{S_t}{S_w} = -C_{L_{t_{\alpha_t}}} L_h \frac{\dot{\theta}}{V}\frac{L_h}{c}\frac{S_t}{S_w}$$

and expressing $\dot{\theta}$ as $\frac{2V}{c} D\theta$ and $\frac{2L_h}{c}$ as l_h gives

$$C_m = -C_{L_{t_{\alpha_t}}} \frac{l_h^2}{2}\frac{S_t}{S_w} D\theta$$

The contribution of the wing depends on the assumed axis of rotation (center of gravity) but a fair average value will be obtained by assuming that the center of gravity is at the wing quarter-chord point. This assumption gives a value

$$C_m = -\frac{\pi}{4} D\theta$$

The total pitching-moment coefficient due to pitching therefore is

$$C_{m_{D\theta}} = -\frac{\pi}{4} - C_{L_{t_{\alpha_t}}} \frac{l_h^2}{2}\frac{S_t}{S_w}$$

Derivative C_{m_δ}.—The derivative C_{m_δ} may be measured directly in a wind tunnel or may be computed from wind-tunnel data on the value of $C_{L_{t_\delta}}$ for the horizontal tail by means of the formula

$$C_{m_\delta} = -C_{L_{t_\delta}} \frac{l_h}{2}\frac{S_t}{S_w}$$

Derivative $C_{m_{D\delta}}$.—The derivative $C_{m_{D\delta}}$ may be computed from

$$C_{m_{D\delta}} = -\left[\left(\frac{\partial C_L}{\partial D\delta}\right)_A + C_{L_{t_{\alpha_t}}}\left(\frac{\partial C_L}{\partial D\delta}\right)_B\right]\frac{l_h}{2}\frac{S_t}{S_w}\frac{c_t}{c}$$

where $\left(\frac{\partial C_L}{\partial D\delta}\right)_A$ and $\left(\frac{\partial C_L}{\partial D\delta}\right)_B$ may be obtained from figure 1 of reference 11, which is based on thin-wing potential-flow theory.

Derivative $C_{h_{D\theta}}$.—The derivative $C_{h_{D\theta}}$ is given by

$$C_{h_{D\theta}} = C_{h_{\alpha_t}} l_h$$

In the absence of viscous friction in the elevator control system, the value of $C_{h_{D\delta}}$ may be computed from

$$C_{h_{D\delta}} = -\left[\left(\frac{\partial C_h}{\partial D\delta}\right)_A + C_{L_{t_{\alpha_t}}}\left(\frac{\partial C_h}{\partial D\delta}\right)_B\right]\frac{c_t}{c} \qquad \text{(A1)}$$

where $\left(\frac{\partial C_h}{\partial D\delta}\right)_A$ and $\left(\frac{\partial C_h}{\partial D\delta}\right)_B$ may be obtained from figure 1 of reference 11.

If a dashpot, which has a damping constant of K pounds per foot per second and moves a distance of Q feet per radian of elevator deflection, is inserted in the control system,

$$C_{h_{D\delta}} = \frac{4Q^2K}{\rho V S_t c_t c} \qquad \text{(A2)}$$

The total value of $C_{h_{D\delta}}$ is the sum of equations (A1) and (A2).

Derivatives $C_{h_{\alpha_t}}$ and C_{h_δ}.—The derivatives $C_{h_{\alpha_t}}$ and C_{h_δ} can be calculated by thin-wing-section theory but the results are of doubtful accuracy because of three-dimensional and boundary-layer effects. It is therefore best to obtain these derivatives from wind-tunnel tests.

APPENDIX B

CALCULATION OF NORMAL ACCELERATION DUE TO OSCILLATING ELEVATOR

The normal acceleration of the airplane, which is equal to $D(\alpha-\theta)$ in nondimensional units, can be calculated from

$$\frac{D(\alpha-\theta)}{\bar{\delta}} = \frac{-C_{m_\delta}C_{L_\alpha}-C_{L_\alpha}C_{m_{D\delta}}\eta i}{2\left[-\frac{C_{m_{D\theta}}C_{L_\alpha}}{2}-2A_w\mu C_{m_\alpha}-\eta^2(4A_w{}^2\mu^2k_y{}^2-C_{m_{D^2\alpha}}2A_w\mu)+i\eta\left(-2A_w\mu C_{m_{D\theta}}+2A_w\mu k_y{}^2\frac{C_{L_\alpha}}{2}-2A_w\mu C_{m_{D\alpha}}\right)\right]} \tag{B1}$$

where η is the angular frequency of the elevator.

The fraction in equation (B1) can be reduced to an ordinary complex number and the modulus of this number is the maximum amplitude of the steady oscillation. The value can be converted to physical units by the formula

$$\text{Normal acceleration per } g \text{ Stick friction in pounds} = \frac{4I_x r}{\rho S_e c_e c g}\frac{D(\alpha-\theta)}{\bar{\delta}}\frac{4}{\pi\eta C_{h_{D\delta}}}$$

where $C_{h_{D\delta}}$ is the value of elevator damping required for the condition of neutral dynamic stability.

REFERENCES

1. Jones, Robert T., and Cohen, Doris: An Analysis of the Stability of an Airplane with Free Controls. NACA Rep. No. 709, 1941.
2. Phillips, William H.: A Flight Investigation of Short-Period Longitudinal Oscillations of an Airplane with Free Elevator. NACA ARR, May 1942.
3. Phillips, William H.: Effect of Spring and Gravity Moments in the Control System of the Longitudinal Stability of the Brewster XSBA-1 Airplane. NACA ARR, April 1942.
4. Jones, Robert T., and Kleckner, Harold F.: Theory and Preliminary Flight Tests of an All-Movable Vertical Tail Surface. NACA ARR, Jan. 1943.
5. Greenberg, Harry, and Sternfield, Leonard: A Theoretical Investigation of the Lateral Oscillations of an Airplane with Free Rudder with Special Reference to the Effect of Friction. NACA Rep. No. 762, 1943.
6. Kleckner, Harold F.: Flight Tests of an All-Movable Vertical Tail on the Fairchild XR2K-1 Airplane. NACA ACR No. 3F26, June 1943.
7. Jones, B. Melvill: Dynamics of the Airplane. The Equations of Motion with Solutions for Small Disturbances from Steady Symmetric Flight. Vol. V of Aerodynamic Theory, div. N, ch. V, secs. 22–31, W. F. Durand, ed., Julius Springer (Berlin), 1935, pp. 135–141.
8. Gilruth, R. R.: Requirements for Satisfactory Flying Qualities of Airplanes. NACA Rep. No. 755, 1943.
9. Gates, S. B.: Proposal for an Elevator Manoeuverability Criterion. Rep. No. Aero 1740, British R. A. E., June 1942.
10. White, Roland J.: A New Method of Longitudinal Control for Aircraft by Use of an Adjustable Angle of Attack Balance. Jour. Aero. Sci., vol. 10, no. 5, May 1943, pp. 152–160.
11. Cohen, Doris: A Theoretical Investigation of the Rolling Oscillations of an Airplane with Ailerons Free. NACA Rep. No. 787, 1944.

U. S. GOVERNMENT PRINTING OFFICE: 1947

E R R A T U M

NACA REPORT No. 791

A THEORETICAL INVESTIGATION OF LONGITUDINAL STABILITY OF AIRPLANES WITH FREE CONTROLS INCLUDING EFFECT OF FRICTION IN CONTROL SYSTEM

By Harry Greenberg and Leonard Sternfield

1944

Page 2, column 1, sixth line from bottom: The missing term on the left-hand side of the equation should be i_s.

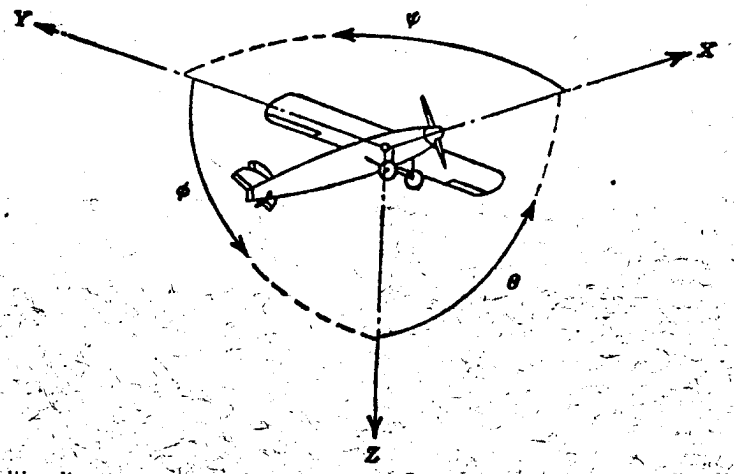

Positive directions of axes and angles (forces and moments) are shown by arrows

Axis		Force (parallel to axis) symbol	Moment about axis			Angle		Velocities	
Designation	Symbol		Designation	Symbol	Positive direction	Designation	Symbol	Linear (component along axis)	Angular
Longitudinal	X	X	Rolling	L	Y → Z	Roll	φ	u	p
Lateral	Y	Y	Pitching	M	Z → X	Pitch	θ	v	q
Normal	Z	Z	Yawing	N	X → Y	Yaw	ψ	w	r

Absolute coefficients of moment

$C_l = \frac{L}{qbS}$ (rolling) $\quad C_m = \frac{M}{qcS}$ (pitching) $\quad C_n = \frac{N}{qbS}$ (yawing)

Angle of set of control surface (relative to neutral position), δ. (Indicate surface by proper subscript.)

4. PROPELLER SYMBOLS

D Diameter

p Geometric pitch

p/D Pitch ratio

V' Inflow velocity

V_s Slipstream velocity

T Thrust, absolute coefficient $C_T = \frac{T}{\rho n^2 D^4}$

Q Torque, absolute coefficient $C_Q = \frac{Q}{\rho n^2 D^5}$

P Power, absolute coefficient $C_P = \frac{P}{\rho n^3 D^5}$

C_s Speed-power coefficient $= \sqrt[5]{\frac{\rho V^5}{P n^2}}$

η Efficiency

n Revolutions per second, rps

Φ Effective helix angle $= \tan^{-1}\left(\frac{V}{2\pi r n}\right)$

5. NUMERICAL RELATIONS

1 hp = 76.04 kg-m/s = 550 ft-lb/sec

1 metric horsepower = 0.9863 hp

1 mph = 0.4470 mps

1 mps = 2.2369 mph

1 lb = 0.4536 kg

1 kg = 2.2046 lb

1 mi = 1,609.35 m = 5,280 ft

1 m = 3.2808 ft